Sapienza University of Rome

ARCHMAT

(ERASMUS MUNDUS MASTER IN ARCHaeological MATerials Science)

Laurea Magistrale in Scienze e Technologie per la Conservazione dei Beni Culturali

Provenance and archaeometric analysis of late Roman glass from the Palatine Hill

Yuliia Storozhylova

Prof. Gabriele Favero (Sapienza University of Rome)

Prof. Paolo Carafa (Sapienza University of Rome)

Dr. Pedro Barrulas (University of Évora)

Rome, October 2019

TABLE OF CONTENTS

ABSTRACT iii
ACKNOWLEDGEMENTS iv
GENERAL INTRODUCTION 1
1. Introduction 1
2. Glass 3
2.1.Chemistry of glass 3
2.2. Brief history and of Roman glass production and some production details 5
3. The archeological context 6
3.1.The history of the Palatine Hill 6
3.2. Excavation of Horrea Vespasiani 15
4. Materials and Methods 19
4.1. An overview of glass shards assemblage. 19
4.2. Analytical techniques 23
4.2.1. X-ray Fluorescence (XRF) 23
4.2.2. Laser Ablation Inductively Coupled Plasma Mass Spectrometry (LA–ICP–MS) 24
5. Results 26
5.1. XRF results 26
5.2. LA-ICP-MS results 32
6. Discussion 38
7. Conclusions 51
Bibliography 52
Annex 55

ABSTRACT

The aim of this thesis was to perform an archaeometric study of the collection of glass fragments, found during excavation of layers dated 6^{th}-7^{th} century AD of a room XII, 1 of the Horrea Vespasians, a complex of warehouses during the Imperial period on the Palatine Hill. These glass fragments were excavated only in 2017 and this is the first study that involves them. A non-destructive approach to study elemental composition of the fragments was chosen. A characterization of the glass fragments was performed by XRF and LA-ICP-MS. In this study, an attempt to reconstruct the production process with possible raw materials and colorants used was made. The results obtained in this study will contribute to the literature on Roman glass production.

ACKNOWLEDGEMENTS

This work was made possible with help and support of numerous people. I would like to take this opportunity in order thank them.

I would like to express my sincere gratitude to my supervisor Prof. Favero and co-supervisors Prof. Carafa and Dr. Barrulas for sharing their deep knowledge of the researched topics and for their support during the whole period of thesis writing. I would like to also thank them for fighting the bureaucracy in a way of obtaining the materials for the analysis with me and for their input to make the thesis better.

I am deeply thankful to Prof. Balossi for finding the samples for this study and helping to create this project on the first place.

I would like to thank Prof. Ridolfi, who provided a possibility to use the XRF instrument in his diagnostic lab for the objects of cultural heritage “Ars Mensurae” and for his support and interest in this study, as well as sharing his knowledge of the topic.

My sincere gratitude goes to Department of Physics and Geology, University of Perugia, and Dr. Maurizio Petrelli in particular for making the LA-ICP-MS analysis possible for this study. Your help in the analysis and the data treatment were crucial for this work.

I am also thankful to the Superintendence for Archaeological Heritage and to the Archaeological Department of Sapienza University for allowing the archaeometrial study of glass fragments collection and Chiara-Luna Fanelli for our meetings and the information about the fragments provided.

All the professors of the ARCHMAT consortium, who have been a part of my education which led to writing this thesis are kindly acknowledged.

My deepest gratitude goes to my closest people: my mom and my sister Nataliya and to Pauel for their long-distance tireless emotional support and for being my source of inspiration and inner strength.

I would also like to thank my ARCHMAT friends and colleagues, who shared their knowledge and supported me emotionally during my thesis semester. I would also like to acknowledge Silvia and Roshan for always staying in-touch and sharing their writing experiences and tips as well as for their care and support.

GENERAL INTRODUCTION

Archaeological artifacts give to humanity an opportunity to explore our past, which often cannot be learned from any other sources. That is why the highest priority of a researcher is to obtain us much information, as possible (while minimizing the harm to the object) in order to gain the full cultural and historical background. Decades before, archeologists and anthropologists used to work on the sites and later, with artifacts, describing and classifying them comparing to already studied ones, nevertheless without having a proper equipment to analyze it. Nowadays, a lot of analytical techniques are available in the arsenal of a researcher. It should be mentioned that the best results can be achieved only with inter- and multidisciplinary approaches to study artifacts. Such studies as dating, chemical or elemental composition, provenance of raw materials are significant in the way of getting a good understanding of an archaeological object, and they cannot be performed by pure archaeologist or historian. In these cases scientists are needed in order to work with the equipment to obtain any results. However, it's also hard for a pure scientist to analyze an archeological object without understanding of its background and choosing the most reasonable and informative way of preforming analysis. That is why the field of archaeometry is developing and broadening with each year.

Often, one of the key points of analysis of an artifact is to preserve it (not only for future studies), because the analyzing object is a piece of human legacy, once destroyed, it cannot be replaced. That is why the damage done to the artifact should be minimal, and non-destructive or micro-invasive techniques are developing and increasing in their popularity. When dealing with a small sample, the choice of the techniques should be performed carefully, with stressing on their non-destructivity in order to save it for a display on a museum or further investigation with other techniques.

Analytical techniques applied to the archaeological object should be used if they could give an answer to the question of researchers, for example on these ones: what is the elemental composition of this object, what raw materials were used, where did they came from and what was the technique of production of the object, etc. Such questions are suitable for glass materials.

1. Introduction

The periods of change always represented a particular interest for historians, archaeologists and various scholars. This is why Rome of 4th - 8th centuries in its decay of glory, population and manufacturing is still magnetic for the researchers. This period of decline has such tragic milestones as the Fall of the Western Roman empire in 476 CE, sacks of Rome by Goths and Vandals in the first part of 5th century, Gothic War in the middle of the 6th century and visit of Emperor

Constans II, who stripped the buildings of Rome of their ornaments and metals in 663CE in order to bring them to Constantinople. The evidences of those and many other events still can be found in the place where the history of Rome is naturally recorded, layer by layer – on the Palatine Hill.

The excavation of the Palatine Hill have brought enormous amount of archaeological materials and shed the light on the life of Romans, especially during the imperial age, late antiquity and the Middle Ages.

This thesis will focus on vitreous materials found during excavation of Horrea Vespasians, which served as the complex of warehouses during the Imperial period on the Palatine Hill. The room XII, 1 of the Horrea Vespasians is a square-shaped space with the sizes of 5x5m with 7 archaeological phases. It should be noted, that the phases are corresponding to the four periods of use, each with a different functionality of the room. Numerous glass materials had been found throughout these periods, represented mostly as shards of open-shaped and close-shaped vessels and rarely as pieces of mosaics. However, none of them were previously analyzed with analytical techniques. Apart from the glass shards, various pieces of non-vitreous vessels fragments with some surfaces covered with glass have been found during the excavation as well. Archaeologists presume that these objects might be attributed to the glass production.

For the archaeometric study of glass materials a non-destructive and a micro-invasive techniques were chosen: X-ray fluorescence (XRF) and laser ablation inductively coupled plasma mass spectrometry (LA-ICP-MS). XRF technique was selected to study bulk chemical composition and major elements and LA-ICP-MS - a micro-invasive technique that was chosen for a study of major and trace elements, which will be used to study the provenance of glass fragments.

In order to design a provenance study one of the first steps of the research will be finding the possible sites with sand and natron used for the glass production during the late antiquity. The work with historical documents is essential in order to locate the places of origin of raw materials.

This study is determined to answer following archaeological questions: Do the fragments have the same place of origin of their raw materials? Is there a change in raw materials used thought the time or it is random? Was it the secondary glass that was made elsewhere, but shaped into a final object locally or the whole glass production of fragments was local? Is it possible to determine were the fragments made by recycling glass?

The data from chosen non-destructive and micro-invasive techniques can answer the abovementioned question. This thesis will focus on three main research aims:

1) An origin of glass fragments and their raw materials;
2) A technology of glass production;
3) A study of colorants and opacifiers used for the glass production;

2. Glass

2.1.Chemistry of glass

Glass can be defined as a non-crystalline solid material, which is usually obtained by cooling from a liquid phase omitting crystallization.

The most familiar, and historically the oldest, types of glass are "silicate glasses" based on the chemical compound silica (silicon dioxide, or quartz).

In the Fig.1 the main structural difference between an SiO_2 glass and an SiO_2 crystal can be easily seen. A structure of glass, as opposed to a SiO_2 crystal does not possess a long-range periodicity. In the crystal the primary tetrahedral units are geometrically and periodically ordered in a regular network, while in the glass such units are randomly distributed, forming a distorted network.

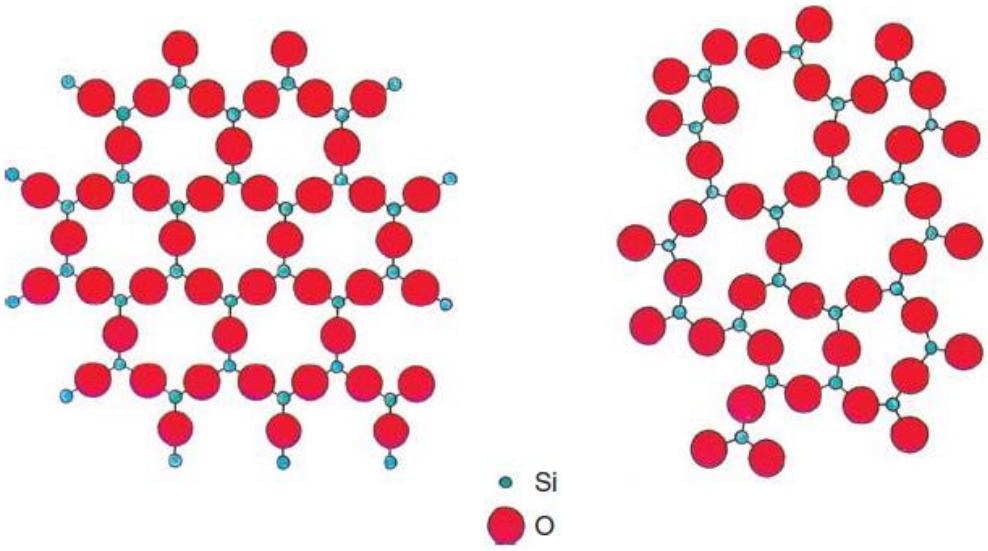

Fig. 1. A structure of a crystalline ordered SiO_2 and a random network of a pure SiO_2 glass[1].

There are several substances that are necessary for glass formation, such as former, flux, stabilizers, fining agents and intermediates. Such substances as opacifiers, colorants and decolorants can be optionally added to the glass matrix, enhancing the resulting glass appeal.

Former, sometimes referred in the literature as vitrifier, is probably the most important part of glass, as it forms the matrix of the glass. Silica is the most common vitrifier used. During Roman times silica was obtained from sands by making quartz powder through grinding quartz rocks or pebbles.

Apart from the silicon dioxide the sand used for glass-making also contained such impurities as:

- Lime, a mineral that contains calcium in forms of an oxide (CaO) and/or hydroxide ($Ca(OH)_2$);
- Calcite ($CaCO_3$);
- Alumina (Al_2O_3);
- Magnesia (MgO);
- Iron oxide (Fe_2O_3), which is also acting as a glass colorant.

However, the chemically pure SiO_2 has a melting point of 1723°C which was unreachable during the Roman period. Even with some abovementioned impurities, the sand used for glass making still had an extremely high melting temperature. Therefore, an elegant solution was chosen– to add a component – a flux, to simplify the process.

Fluxes are used in glass-making because they lower the melting temperature of an mixture of solid compounds. [1].With the flux addition to silica the glass can be made in a kiln with the temperature near 1200°C. A substance called "soda" – sodium carbonate (Na_2CO_3) was commonly used as a flux. Soda was obtained from natron, a salt found in dry lake beds. During the Roman period, most of the natron was coming from Wadi El Natrun[4], located in Egypt. However, there is a possibility that there was a source of natron in Italy too. Apart from natron, plant ash and wood ash were also used as fluxes during the history of glass-making.

Nevertheless, with the addition of a soda to pure silica the problem of solubility is arising, because a glass formed of just these two substances is naturally soluble. Thus the addition of a stabilizer such as lime or magnesia is required. However, these substances have already been described by the author as impurities entering the mixture with the sand, instead of a component added by Romans in purpose.[5]

Fining agents are components that are added to glass in order to help removing glass bubbles and thus making the glass more homogeneous. Various sulfates and chlorides impurities present in the raw materials, as well as KNO_3 and MnO are the main fining agents. [1]

Intermediates have an intermediate electronegative character between vitrifier and flux. They can substitute Si in tetrahedral structures of the existing network. Those elements are Al, Ti and Zr. [1]

The color of the glass is obtained due to the presence of transitional metal ions or metallic atoms present in the structure. The resulting color depends on the oxidation state of the element.

Main ancient colorants are manganese (more than 0.8 wt%) for purple (Mn^{3+}) and brown (Mn^{2+}), cobalt (Co^{2+}) for blue; irons for yellow to brown (Fe^{3+}) and green and blue color (Fe^{2+}); copper oxides for green and blue (Cu^{2+}) and red color (Cu^{+1}, Cu^{0}); silver for yellow to brown color (Ag^{+}); gold for red; and a mixture of gold and silver for obtaining pink glasses. In case if the higher quantity of iron oxides introduced into the glass as an impurity, results in unwanted colors, such as green, blue and yellow-brown hues in particular, it could be removed by adding decolorants. Main decolorant of a Roman period is manganese oxide (0.3/0.5 – 0.8 wt%). [1]

Opacifiers were used to make the glass opaque. Calcium antimonite ($Ca_2Sb_2O_7$), tin dioxide(cassiterite; SnO_2), lead stannate (Pb_2SnO_4; $PbSnO_3$) and lead antimonite ($Pb_2Sb_2O_7$) were mostly used as opacifiers.

It should be also noted that chlorine in Roman glasses coming from NaCl as a contaminant in the natron.

2.2. Brief history and of Roman glass production and some production details

During Roman times two main technologies of shaping the glass such as casting or glassblowing. Glassblowing was invented in the 1st century AD and made a revolution in how the glass objects were made[6]. However, with the glass production from the raw materials to the final object, we have a bit more complicated scheme. It is strongly supported by the archaeological evidences that the glass in the Roman Empire of our era was mostly produced in Egypt and Siro-Palestinian areas, where the most famous natron sources were. Most of the researchers are sure that Wadi el Natrun, c. 50km northwest of Cairo, Egypt and at al-Barnuj, Egypt were main natron sources for the Roman glass[8-11]. The silica and lime sources could be local.

There were three ways of producing a colorless glass in Roman times:

1) by selecting a high quality raw materials

Natron composed mostly of sodium compounds, having a low level of impurities and silica sand that probably was chosen carefully in order to not introduce more impurities into the resulting glass [7] ;

2) by adding a decolorizer

Antimony and Manganese decolorize glass by oxidizing the iron (Nevertheless, it should be noted that the relationship between Fe, Mn and other glass' compounds is quite complex). According to Pliny, sand from the Volturno river was used for colorless glass production;

3) accidentally

For example, when Mn came with sand, as it was in cases of sands from Egypt and Volturno river.

A colorless glass can be produced either by selecting raw materials that are low in iron or by the addition of a decolorizer to the glass.

In 1961, Sayre and Smith suggested a model for the use of decolorizers in Roman colorless glasses. They found that colorless glasses from the Syrian coast are characterized by the increasing use of manganese oxide (MnO) rather than antimony oxide (Sb_2O_5), in concentrations in the order of 1% MnO towards the end of the Roman imperial period. The model of Sayre and Smith has since been used extensively to characterize the use of decolorizers in colorless glasses throughout the Roman Empire [16-20] Later works by Sayre and Smith revealed that in Italy and northern Europe, glasses were usually decolorized with either antimony or antimony/manganese until the end of the 3rd century AD[21][22][23]. After that, a growth in manganese content appears, which is deduced as the deliberate addition of decolorizers, when reached above 0.2%.

3. The archeological context

3.1.The history of the Palatine Hill

Regio X Palatium coincides with Palatine Hill. This area, between the Tiber and Velian, Caelian and Aventine Hills is the heart of the city and the place of Rome's foundation. In the beginning, it prolonged only over Palatine Hill. Powerful established their residence on the *Palatium*: from the founder Romlus's hut to the deluxe *domus* of the magistrates of the Republic, to the imperial palaces that extended to the point that they occupied the entire hill.

Since that time, the term *Palatium*, meaning Palatine Hill, has meant "palace". What remains of the long-lasting history of this part of Rome, can be found today within a unified archaeological area. It should be mentioned, that the medieval and modern development of the city never involved Palatine Hill, whose monuments slowly decayed and crumbled to the ruins that mark it today.

Beginning in the fifth century, the only inhabited part of the palace called *domus Augustiana* was on the top of the hill. The surrounding infrastructure on the slopes of the hill were abandoned and in the end, slowly but surely, were buried. Years later, a small necropolis arose from several previously separated burials, marking the radical transformation of the landscape.

, There is no trace of habitation remains, on Palatine Hill in the Middle Ages except for the northern slope. Only in 16th century several noble families began to build villas in the hill's vineyards. [12]

These families occupied the rest of Palatine Hill between the 16th and 18th centuries. The first excavations started in the 16th century by the property owners, however all the findings end up in private collections and market of antiquities.

Between 1720 and 1726, the first systematic excavations were carried out in the *Domus Augustiana*, ordered by the Duke of Parma, Francesco I, who at that time owned the Horti Farnesiani. Francesco I made Prelate Francesco Bianchini director of the excavations. During these excavations aula Regia was uncovered, along with the statues it housed - Hercules and Dionysius in green marble, now in the National Gallery of Parma. [12]

The first evidences of the Palatium inhabitance, according to Dionysius of Halicarnassus, where during the time the Palatine was the distant part of the kingdom held by chief of Siculi, Cacus. As one of the earliest evidences of his rule are stairs named after him, the *scalae Caci*. Above them his household was situated together with a shepherds' village, probably dedicated to his sister *Caca*. Around 1253BC, Cacus was dethroned by the Greek Evander, and his colonists from Arcadia, who settled on Palatine Hill and named it *Pallantion*. Evander founded the settlement and brought the cults of deities such as *Nike-Victoria* and *Pan Lykaios-Faun* on Palatine Hill. According to the legend the leader of a second Greek expedition from Argolis in 1235BC – Hercules murdered Cacus, consequently ending the war between chiefs. According to Virgil a third Greek expedition reached the northern slopes of Palatine hill, they moved alongside the palace of Evander, which served as a home for the future rulers. [12]

Later phases of settlement in Palatine Hill were happening in the historical epoch, which provides more evidences about the occupation of Palatine Hill.

During Latium phases I-IIA1, corresponding to 1050-900BC a village of Velienses was probably situated on the *Palatium*, which is confirmed by archaeological evidences from that time – ceramic materials from the Cermalus and partially preserved huts and a burial of a child with a wooden casket on the northern slope. [12]

The Latium phases IIA2 –IIIA (900-825/775BC)

This period marks the proto-urban period of Palatine Hill. It is during this period *Palatium* becomes more significant in comparison to other hills. The settlement has its districts and curiae on each of three hills – *Palatium*, *Cermalus* and *Velia*, but the celebrations are carried out on Palatine

and Velian hills. Later, the settlement expanded to Caelian and Esquiline Hill , thus creating a system of *montes*, which eventually include *colles* and was referred as *Septimontium*. This proto-urban cluster of settlements resided twenty-seven *curias*. [12]

Late Kingdom (616-509 BC)

This period marks several important landscape changes due to public works made by Tarquins, that were crucial to the development of Rome. They included the draining of *Velabrum* and *vallis Murcia*, which removed the natural barrier of western and southern sides of the Palatine Hill. Rivers that flow to the north, between Palatine and Velian Hills were controlled with a help of leeves, made in masonry. However, one of the courses of the water flow was redirected to an underground channel at the beginning of 6th century BC, which drastically changed the landscape. In this particular period, the first substructure thick walls made of tuff were build, which changed the difference in elevations into artificial terraces. During this period of time in the southeastern part of the Palatium a sacred area was established. It endured for a long time.

Apart from that, there are evidences of the city expansion as both *cilvus Palatinus A* and *B* extended beyond downhill that *via Sacra.* On the southern side of the road five *domūs* (built *circa* 530BC) organized in two city blocks were excavated.

The early Republican age (509-396BC)

During this period of time there are no evidences of major modifications of the city zones on the Palatine Hill. Residential and sacred areas from the previous periods have evidences of continued use. The literary sources indicate that Palatine Hill was an exclusive residential area. [22]

Mid Republican age (396-240 BC)

In 396 BC the conquest of the city of Veii, have brought to Romans new sources of their main building material – tuff. The sources of this yellow tuff were located along the Tiber valley. This material was later used for building walls incorporated into the southeastern walls erected in previous periods, thus supporting a terrace and changing the landscape into artificial. [23]

In 390BC Rome was sacked by Gauls, during which most areas of *Cernalus* were burned down. After the event, a reorganization of the zones which suffered a fire was done, which elevated the ground level for 1,5 m above sea level, reaching 40,5 m a.s.l.

This period marks several important changes of the sacred area at the top of the Palatine Hill. On the one hand, some archaeological evidences indicate that the temple was rebuilt with different dimensions, and that area was in use until 1st BC. On the other hand, the materials

extracted from wells are attributed to households, thus marking the appearance of several houses in the former sanctuary area. [24]

There are evidences of restructuring of the *domūs* from previous periods, on the northern side of the hill. [12]

Late Republican age (240-36 BC)

This historical period has several important milestones, such as Second Punic War. In the beginning Late Republican age of A cult dedicated to Magna Mater was strengthened in Rome because of an omen, which resulted in a diplomatic mission to Pessinus to retrieve the *simulacrum* of the goddess, the sacred black stone. [12] It was kept in the Palatine temple of Victoria until the *aedes Magnae Matris* was completed in 191 BC. Annual plays had been made in the honor of the goddess in a provisional theatre and soon the permanent theatre was built on the Palatine Hill.

During this period a residential block with at arose near the sanctuary, beyond the *scalae* Caci, surrounded by tuff walls. It is believed that Octavian lived there [25].Three different *domūs* of the same period where identified to the north, south and on the southern slope of Palatine Hill. Another residential sector has been founded on the side of the hill facing *Velabrum*, behind the Sanctuary of Victoria and Magna Mater. Circa 125 BC an elite residential area existed on the Palatine Hill, as confirmed by Gaius Sempronius Gracchus, who preferred to change his habitation place to Forum in order to be closer to the people. [26]

In 210 BC a part of the city between via Sacra and the Forum suffered a huge fire, which was probably the cause of following significant construction activities in the area between *cilvus Palatinus A* and *B* by the end of 3rd century. [27]

By circa 150 BC on the slope facing the Caelian Hill a temple of *Fortuna Respiciens* was constructed. [28]

In 111 BC there was another fire that broke out of the residential areas reached the Temple of *Magnae Matris*. [29]The sanctuary was not only reconstructed, the surrounding architectural ensemble was rearranged. The foundation was built in front of the sanctuary. The tuff walls from previous epochs were strengthened and enclosed with the Roman concrete and reticulate, functioning as a substructure for the constructions on the top the hill.

Regarding the charges in the residential area, three blocks of houses were built beyond the scalae Caci at that period of time. Several *domos* attributed to the noble families in different residential quarters were also reported.

By year 58BC one of the most ambitious projects of residential buildings have been performing – construction of a house for Clodius– the leader of the plebeians at the time and his wife Fulvia. It was scandalous at the time, as he tried to buy the neighboring properties and in case of denial – had the neighbor killed.[30] Clodius even destroyed the bordering public properties, such as porticus Catuli, to construct another building and a panoramic paved walkway 88m long. After that, Clodius used some manipulations in order to obtain a major part of the house of Cicero, who had been exiled to Macedonia. The tribune demolished the peristyle and constructed the monument to a goddess Libertas, and joined the major part of the house to his property. When Cicero has returned from his exile, he found it impossible to share a well with Clodius. However, some rooms of Cloduis domus were demolished due to a system of new walls in Roman concrete and reticulate, and which started another ambitious construction project – building a huge rectangular peristyle and a terrace 88m long. For these projects he was heavily criticized by Cicero in his "pro domo" oration [31]. By 58 BC another ambitious building project was ordered by Marcus Aemilus Scaurus, heir of the domus on of clivus Palatinus B and via Sacra. He placed 4 columns made of black marble to an enormous (459 m^2) atrium [32]. The excavation of the substructure of the abovementioned atrium revealed 62 small vaulted rooms, which were interpreted as quarters of slaves. The property had several domos incorporated, as well as a building with a large garden with a pool and nymphaeum. Consequently, it caught Clodius' attention, who purchased this property in 53BC for 14,8 million sestertii, a sum that Pliny compared to a value of Piramids. [33]

In 53 BC, a few months before his death, Clodius bought another house on the Sacred Way with the largest atrium in Rome, previously belonged to Marcus Aemilius Scaurus. In the following years most of the properties belonged to Fulvia, that had been living her third husband Mark Antony, who delivered the head of Cicero, her enemy, in 43 BC. After the death of Fulvia in 40 BC, the property belonged to Mark Antony and his new wife Octavia.

The archaeological evidences support and clarify the abovementioned events, which changed the cityscape of Palatine Hill at the time.

Augustian age and the early imperial age (36BC – 193 AD)

From 36 BC - 17BC there was a construction of the terraced sanctuary complex beyond *scalae Caci*, consisting of the Temple of Apollo and sanctuaries dedicated to Augustus and Vesta.[35] The first experiments in imperial palaces around the Augustan sanctuary started developing.

The huge property on the slope facing the *Velabrum* that belonged to Mark Antony and his wife Octavia remained empty, after Antony left to Egypt and started an affair with Cleopatra, and

Octavia moved into a house belonging to her brother Octavian. [36] Between 2 and 15 AD Tiberus move in this residential lot. [37] Sometime after that the construction of *domus Tiberiana* has started, and that Tiberius moved in there. Next modifications to *domus Tiberiana* the were made only by Claudius.[38]

It is known from the literature sources that the Temple of Magnus Mater was reconstructed, after damage from a fire in 3 AD[34] A terrace, that was built in the mid-Republican age was strengthened with *opus latericium* masonry. During the beginning of 1st century AD a lot of *tabernae* arose in *Palatium* on *vicus Fabrici* towards Circus Maximus.

On AD 64 a devastating fire broke out of a *tabernae* on the eastern side of Circus Maximus, which quickly spread to the whole Palatine Hill. [39] Only some parts of the *Palatium* facing the *Cernalus* and the *Velabrum* were not affected by this tragical event. The Temples of Victoria and Magna Mater were not reconstructed after the fire, but the Augustian complex is reported to have some external works. During the next four years, some reconstruction works were performed in *domus Publica* by Nero. During his reign, Nero built a *domus Augustiana* on the top the Palatine Hill, probably as an enlargement and extension of the *domus Augisti*. The road leading to the entrance of the palace was rebuild and significantly widened. The palace has an entrance that opened into *area Palatina* – a large plaza, where aristocracy gathered to greet the emperor. During the time of Nero's reign major part of *Palatium* belonged to the emperor and *Area Palatina* serves as a new Forum. The northern slope undergoes a significant change in a cityscape as *domus Aurea* on the Sacred Way arises and a new paved road leading to Nero's palace was built.

The *clivus Palatinus A,* which stretched from via Sacra to the *domus Augusti* had been replaced by *clivus Palatinus B,* which led to the *domus Augustiana*. Its importance will only increase from that point. By the rule of Antonine dynasty, *clivus Palatinus A* will be just a path along *horrea Vespasiani.*

During the reign of the Flavian dynasty (69-96AD) the construction on the Palatine Hill intensified. It is known, that in that time period the imperial palace had been expanded and occupied the whole Palatine Hill. On the side of the *clivus Victoriae* a set of double-level vaulted room, that presumably were used for commercial purposes, were built.

From 68 AD the so-called "seat of power" moved to the *domus Augustiana,* construction of which was started by Nero and completed by Domitian, a son of Vespasian, *circa* 92 AD. During the reign of Vespasian (69-79 AD), *aula Regia* was remodeled and several adjustments were made to the *domus Augustiana.*

Domitian's construction improvements of the *domus Augustiana* during first ten-eleven years of his reign were so impressive, magnificent and tall, that according to some sources, that "the pyramids of Egypt seemed ridiculous in comparison". [40] It is hard to believe, but the height of the main hall reached 30m and the area of the imperial palace extended to 49,000m^2 with only *aula Regia* extending 1,394m^2. During his reign a basilica, which connected *domus Augustiana* and *domus Tiberiana* through tunnels was built and a garden dedicated to Adonis was set.

In the Flavian period, in the area at the foot of the *domus Tiberiana* was a quarter with buildings separated from each other by descending streets which led to a long road with numerous *tabernae*. Between the abovementioned road and via Sacra a huge *horreum* was situated. It was built when Vespasian was the emperor and thus called *Horrea Vespasiani*. *Chronography of 354* mentions the structure identifying is a warehouse. Considering its immense size, absence of internal divisions as well as short distance to the imperial structures *Horrea Vespasiani* is presumed to be a storage of large amounts of *frumentum publicum*. This theory is supported by two inscriptions made by 35 tribes that thank the emperor Titus for the free distribution of wheat. [41]

According to the archaeological evidences [12],in the end of 1st century AD the *porticus* was transformed into the two identical spacious *horrea*. It was built according to the new safety protocol established after the devastating fire in 64 AD and satisfied the necessity in clean and ordered commercial block of the city. [12] Finally, the butchers, barbers, cooks and tavern keepers were not scattered all over Rome, but situated in one place. In the center of each *horreum* was a courtyard with a portico surrounded by shops. Due to the design each square-shaped room has area of 25m^2, and it was possible for the merchants to situate in several rooms, enlarging the overall shop area. Each of the *horrea* had at least two floors, with the ground level at the same height as the portico's entrance of Sacred Way, and the first floor being in the same level as the road along the city block uphill. For the construction of the *horrea* the slope of the hill an excavation under the foundation of Vespasian *porticus* was carried out. It had been done in order to set the same floor level for the whole building. [12] The pillars and arches were strengthened by buttresses for a better support of the first floor.

The first change in the function of *horrea* was during the reign of Dominitian, from the wheat distribution centers they become commercial centers of Rome. It was most probably food oriented *horrea*, and even had several basins for fish that was sold there.

Near the *Horreum A* was an *arcus in summa Sacra via*, an arch with relief portraying Mars and Venus. The street with the arch led onto the crossroads with *clivus Palatinus B,* where Dominitian constructed an arch dedicated to his brother Titus – *arcus Titi*.

During the Antonine period (98-193 AD), to be more specific circa 150 AD the substructures of the corner of the *Palatium* facing the *Velabrum* had been rebuilt, as a wall in *opus caementicium* behind the older wall built in mid-republican period. In addition to serving its primary function as a substructure it also supported the water distribution system made of pipes and cisterns, which supplied most of the imperial complexes with water. [42, 43]

There are evidences of reconstruction of the Temple of Magna Mater and building a podium in *opus caementicium* in the *area Palatina.*

Regarding the *Horrea Vespasiani* during the Hadrian reign, some sections of the walls of the eastern *horreum* being rebuilt as well as 3 basins were added to one of the shops. In the western *horreum* a central portico had been removed and, probably to create more open spaces. Some of the corner pillars were reused and leaned up against a new structure consisting 10 rooms. [12] This new part of the commercial center was accessed through two passages aligned with the main entrance. Via Sacra's sidewalk near the *Horrea Vespasiani* at the time was full of small rooms and monuments.

Mid-imperial period (139-312 AD)

In the Severan period there are evidences of work carried out in *Horrea Vespasiani,* as its western portico was transformed into a footpath that replaced *clivus Palatinus A,* which was removed as a result of an expansion of the House of the Vestal Virgins during Trajan reign. Thus, only an *arcus in summa Sacra via* was left out of the formed road that used to lead to the palaces in the begging of the 1st century AD.

During the reign of Severan constructions mostly involved enlargement of *domus Augustiana* by adding a new long wing called the *Septizodium* to the property. Another building constructed in contact with garden's portico is known as *domus Severiana* was extended in the direction of Circus Maximus.

Late imperial and High Middle Ages (312-553 AD)

Historical sources of that time does not mention the *Horreum Vespasiani,* however the archaeological evidences confirm that it was in use during this period.

There are several changes in the Palatine Hill during this period, that worth mentioning.

First of all, in 394 AD emperor Theodosis prohibited the celebration of paganism, thus the Sanctuary of Victoria and Magna Mater was forced to stop functioning. After the Alaric's sack of

Rome, some areas of the temples have been abandoned, and it other some maintenance work was performed. As the temple of Magna Mater fell into ruins, the temple of Apollo nearby burned in 363 AD, even before the paganism was prohibited. A Christian chapel arose on foot of the sanctuary substructures.

In 455 AD the *domus Augustiana* was stripped of its golden, bronze and other precious objects by Gensric's Vandals. The palaces have suffered the earthquake in between 484-508 AD, and the Ostrogoth king Theodoric that visited the palaces made some works upon the palace's reconstruction.

3.2. Excavation of Horrea Vespasiani

On the plan of the Palatine Hill in 81-96 AD (Fig. 2) Horrea Vespasiani can be found on the north of it, marked with a letter D.

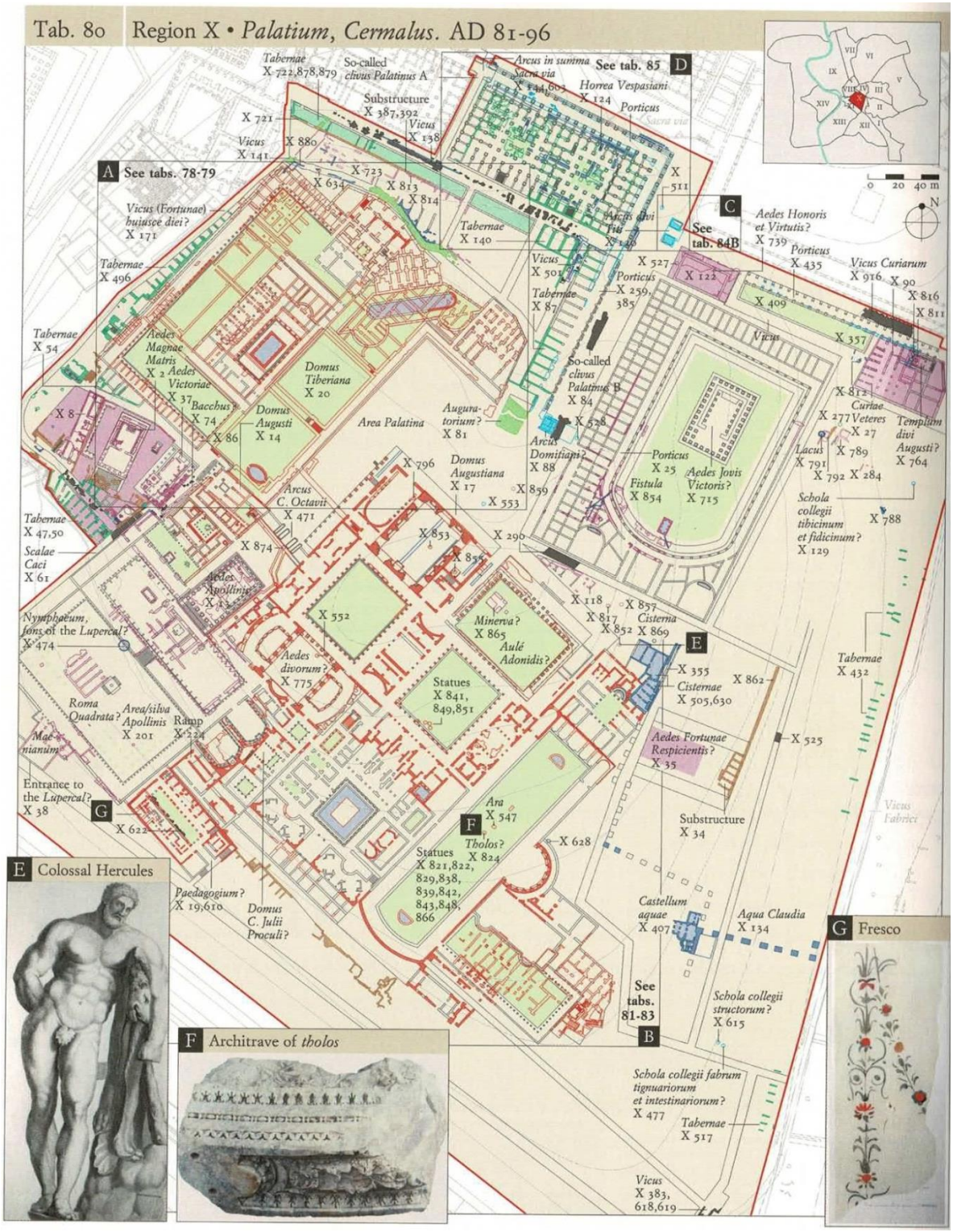

Fig.2 The map of the Palatine Hill during the Imperial Period. Horrea Vespasiani could be seen on the central upper part of the map. [12]

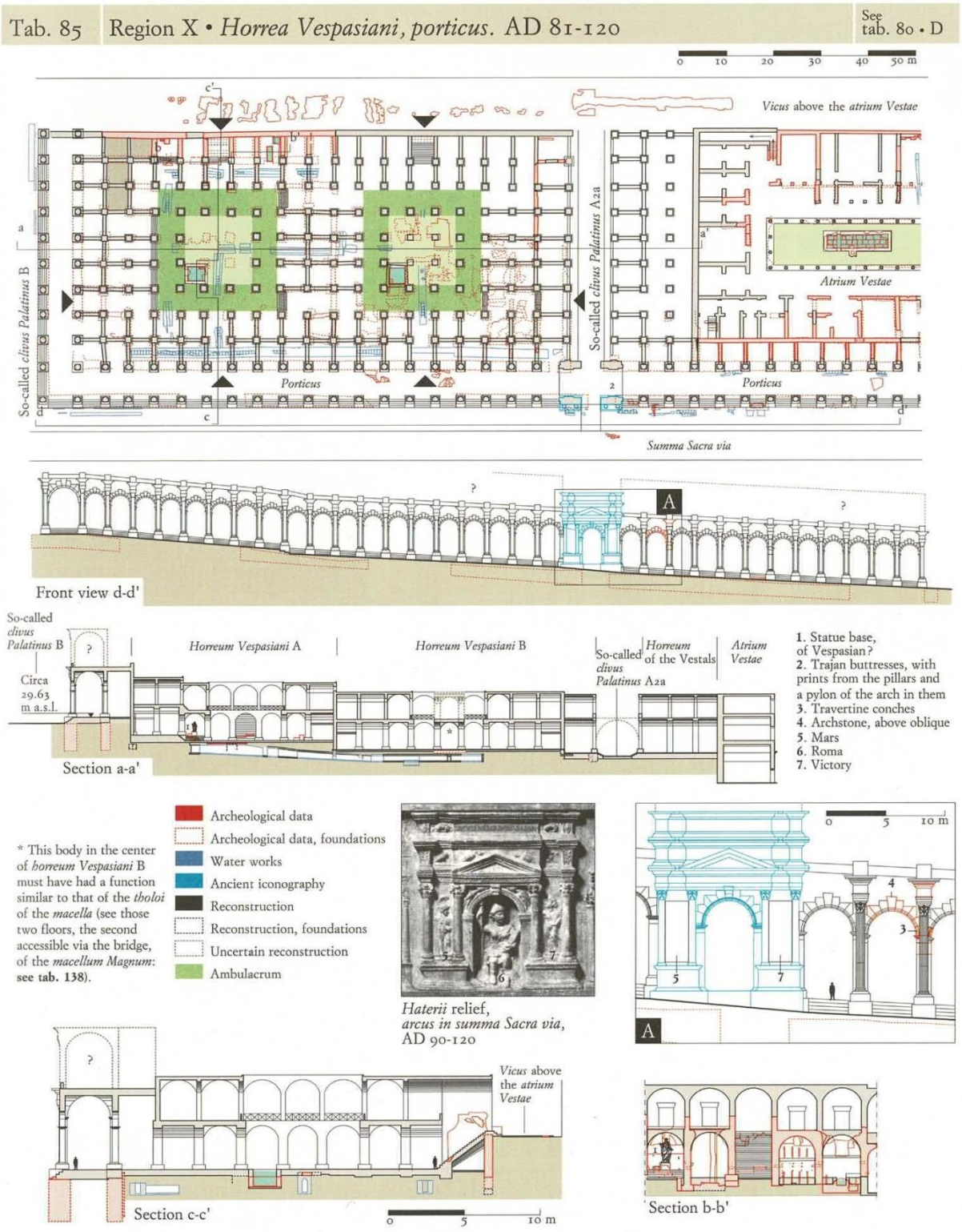

Fig.3 The reconstructed schematic view of Horrea Vespasiani (A and B) from the top and the side, in order to show the construction better. [12]

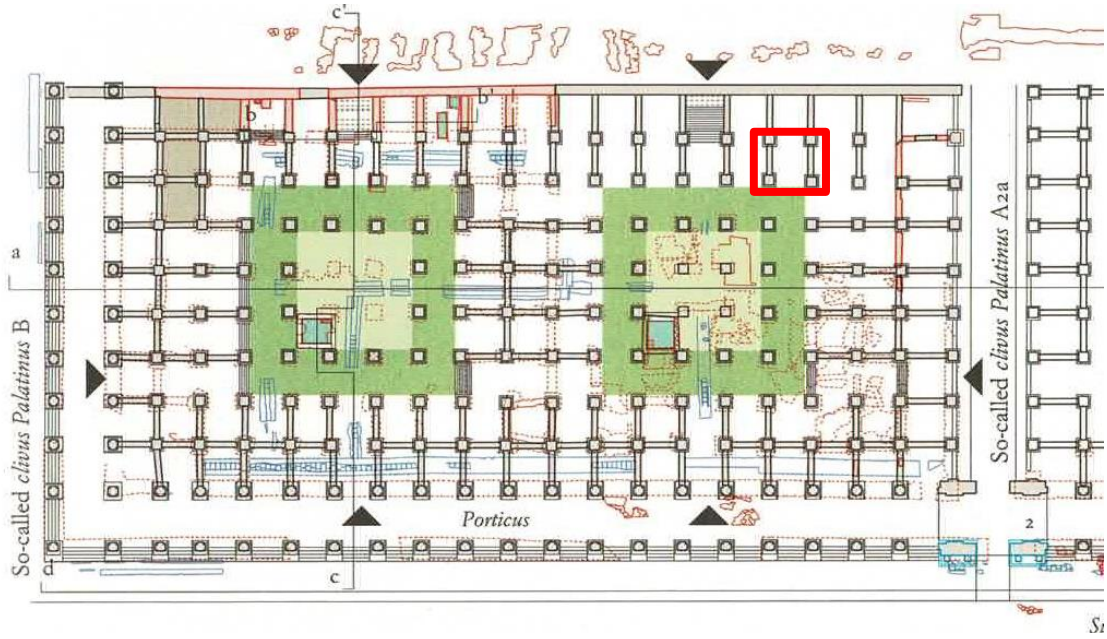

Fig.4 The location of the room (XII, 1) on the plan of Horreum Vespasiani is marked with a red square

Period I (Roman Imperial period). The room (XII, 1) is part of the *Horreum Vespasiani* – a big warehouse for supplies. This quadrangular space has dimensions of 5x5 meters and its floor is made of *opus spicatum* (angular layout of the bricks). The entire structure conducts its primary function.

Period II (Late Antique period). The functionality of the room changes.

1st Phase (second half of 5th AD – beginning of 6th AD). After the its primary use, the room is distraught by destructive activities and obliteration: five little pits are excavated; soon after that the room is filled up with an accumulation of earth and various types of materials. The main composition of these layers seems to be clay and silt. Besides, a thin layer made of semi-liquid glass spreading almost all over the ground of the room has been documented.

2nd Phase (around first half of 6th AD). A new accumulation, mainly made of sand of a natural origin, occurs in the room.

3rd Phase (probably first half of 6th AD, but uncertain due to the absence of pottery to date the phase). During this phase a new type of functional change related to a craftsmanship activity occurs. The craft system was later covered with a vast group of layers made of earth and numerous materials.

4th Phase (first half of 6th AD). The obliteration activities of silt and sand continue. However, this phase has a little pit, which was later filled up with ruins.

5th Phase (during the 6th AD). This phase includes various evidences of craftsmanship activities. The room is filled up with large and small layers, rich in materials. A floor, made of clay and sand, is set right on the pit previously filled with ruins. The floor coincides with overfired layers, that could be an indicator of several fires. An entire fireplace with its pit and overfired clay layers was also found.

Period III (end of Late Antique Period). The functionality of the room has changed again: it becomes a cemetery.

6th Phase (half or second half of 6th AD). New actions of filling were made to level the floor and there are three intact burials. A single skeleton of a child was found in each of the burials. There are two types of burial typology: inside an amphora (*enchytrismos*) and a cappuccina (a sloping covering made of reused bricks and marbles). The tombs have been covered with earth.

Period IV (end of Late Antique Period – beginning of Medieval Period). Another change in the function of the room takes place.

7th Phase (between end of 6th and almost end of 7th AD). The entire room is entirely filled up with an enormous amount of materials mixed up with earth.

The analyzed glass fragments come from the following layers of the excavation of room (XII,1) of Horreum Vespasiani.

36073, 36073 I.M., 36072: **phase 7**. Group of activity **A** (= construction). Activity 24. 36073 is the biggest layer, rich in materials. I.M. stands for Interfaccia Morto, a burial's interface (which belongs to layer 36073, but is considered separately due to a different context of a layer)

36095: **phase 5**. Group of activity **B** (= life). Activity 19. It's the fill of a child burial made up with an amphora.

36098: **phase 5**. Group of activity **B** (= life). Activity 18. It's a sandy layer that fills a pit 36100 and it is poor in materials.

36104, 36108. **phase 5**. Group of activity **A** (= construction). Activity 16. Both of the layers are in direct stratigraphic relation and are rich in charcoal.

36192: **phase 4**. Group of activity **A** (= construction). Activity 10. It's part of a bigger fill made of several layers.

Legend:

Activity means a group of different layers that properly refers to the same type of action

Group of activities means different activities which aim to the same purpose (A,B or C). Groups of activities describes the cycle of a phase (composed of preparation/construction, life and destruction and so on with a new phase).[44]

4. Materials and Methods

4.1. An overview of glass shards assemblage.

The amount of glass fragments recovered from the room (XII, 1) of Horrea Vespasiani is truly impressive and it reaches more than a thousand of glass fragments. Majority of the fragments are still kept in the Palatine Hill storage rooms and it was not possible to sample directly from the archaeological site. Fortunately, approximately 200 samples were stored in the Department of Archaeology of Sapienza University and the author was able to choose the samples for the analysis.

After a thorough discussion and planning glass fragments from each of eleven stratigraphic layers were chosen with a correspondence to the abundance of fragments in each layer. Thus, the layer with the biggest amount of glass fragments would be the one with the majority of the fragments picked for analyses. In such way, the research would be aiming for the best representation of a collection without the analysis of every piece of it. The main criteria were also a good preservation of a glass surface of fragment, meaning heavily altered fragments will not be analyzed and some amount of a flat surface is also required in order to obtain more correct data from the instruments. There were no limitations upon the size of a fragment at that point, since there were no glass shards visibly exceeding 10-12 cm in any of the dimensions (length, width or height).Consequently, as all the criteria were matched, the assemblage of 124 glass fragments of various parts of vessels (mouths, lids, lips, necks ,handles, walls, base parts for open-shaped and foots) was formed.

It should be mentioned, that approximately 65-70% of the initial collection of glass fragments was one layer, referred as 36073. Therefore, majority of our samples were taken from this layer, making approximately 65% of the new collection as well. The diagram shows the number of samples chosen to represent the layers starting from the oldest to the newest layer clockwise. The following table shows the number of fragments per layer.

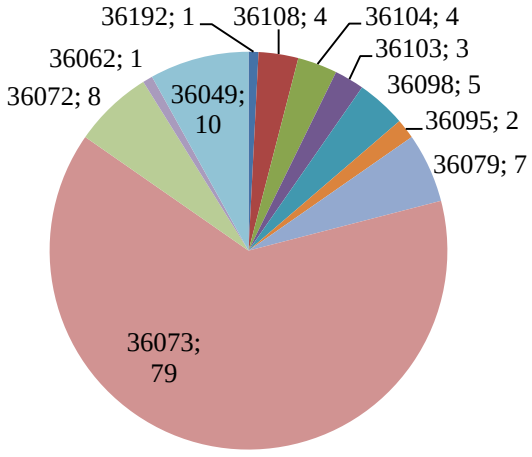

Fig. 5 The diagram showing the number of samples per each layer

Table.1 The amount of fragments per layer

The name of an archaeological layer	The quantity of glass fragments analyzed
36073	79
36049	10
36062	1
36079	7
36098	5
36104	4
36108	4
36192	1
36072	8
36095	2
36103	3

Fig. 6. A photo of the half of the glass fragments, mostly parts of open and closed-shaped vessels from stratigraphic layer 36073 chosen for XRF analysis.

Fig 7. Images of the fragments analyzed with both XRF and LA-ICP-MS (part 1)

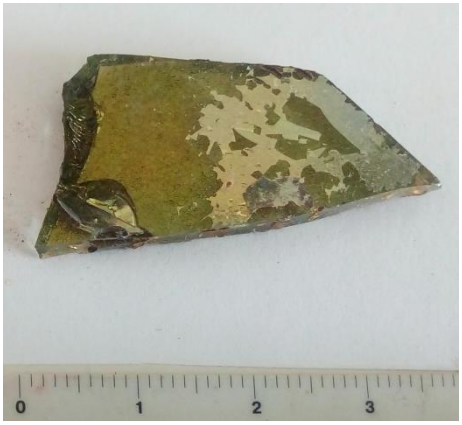
36049_001


36049_002


36049_003

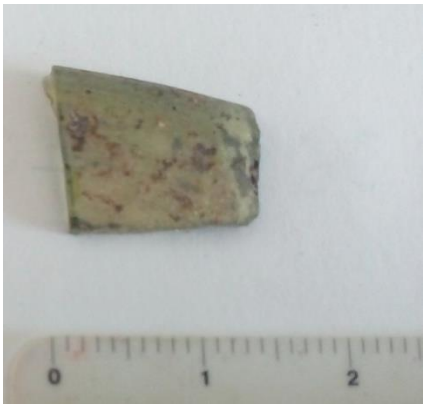
36049_007

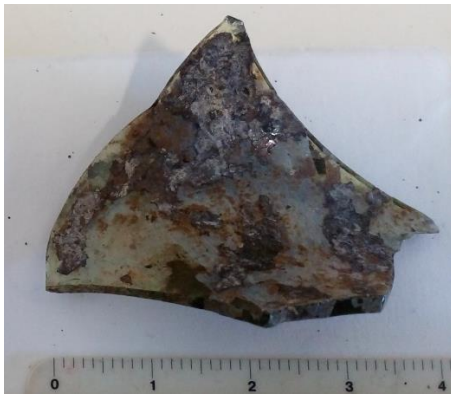
36062_001


36072_001

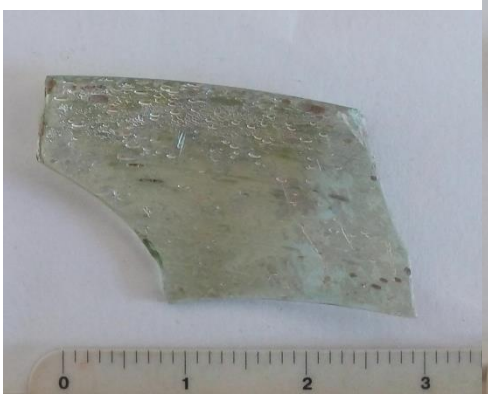
36072_003

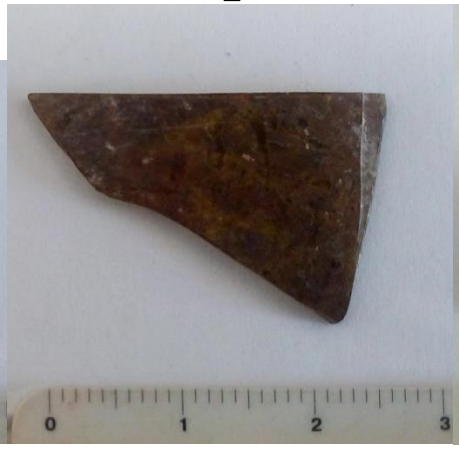
36072_004


36073_046

The first part of a collection of glass fragments on the figure above is represented by:

- four tesserae pieces – 36049_002 (aqueous tint with the iridescence), 36049_003(light blue hue), 36072_001 (colourless with the iridescence layer), 36073_046 (deep blue);
- three rims - 36049_007 (light green tint), 36072_003 (light aqueous tint), 36072_004 (deep yellow-brown)
- one neck of a glass vessel - 36062_001 (green tint with large brown inclusions)
- one body fragment 36049_001 (yellow -green)

Fig.8 Images of the fragments analyzed with both XRF and LA-ICP-MS (part 2)


36073_061

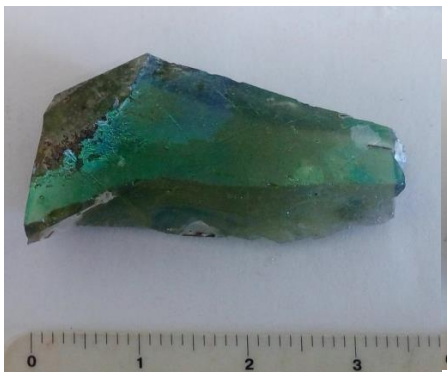
36073_075


36079_003

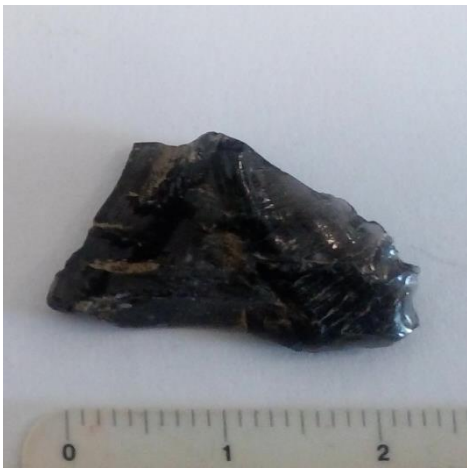
36095_001


36098_001

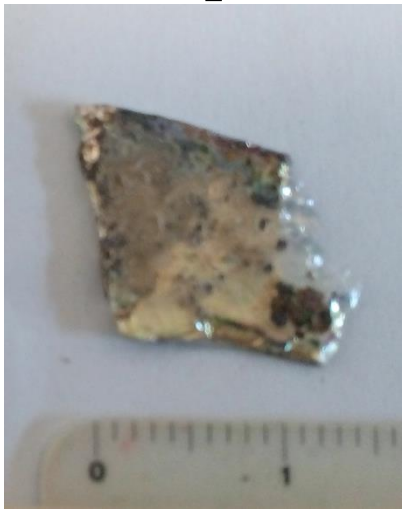
36098_004

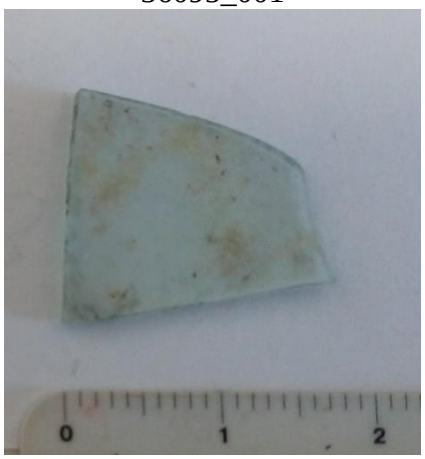
36104_003

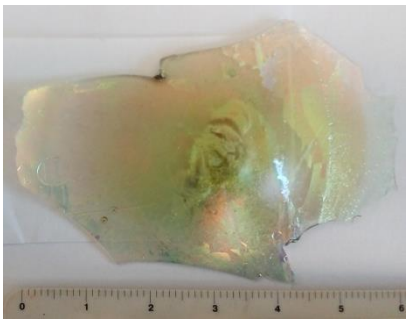
36108_001


36192_001

The second part of a collection of glass fragments on the figure above is represented by:

- one blue opaque handle – 36073_061
- three bases: 36079_003 (opaque with violet-blue tint), 36098_001 (altered with iridescence), 36108_001 (light yellowish tint)
- four walls: 36095_001 (black),36098_004 (altered with iridescence), 36104 _003(light blue tint), 36192_001 (colorless with black inclusions)
- one body part – 36073_075 (grass green colour)

4.2. Analytical techniques

4.2.1. X-ray Fluorescence (XRF)

The working principle of X-ray Fluorescence based on the emission of characteristic X-rays from a sample that has been excited by bombarding with high-energy X-rays.

When an X-ray with enough energy expel the tightly held electrons from the inner shell of an atom, the unstable structure results in a falling of electron in outer orbital into the inner orbital to fill the hole left behind. The energy released accompanied by the falling is equal to the energy difference of two shells. The emitted radiation thus has energy characteristic of the atoms present and the results are expressed as spectra. XRF is widely used for elemental and chemical analysis.

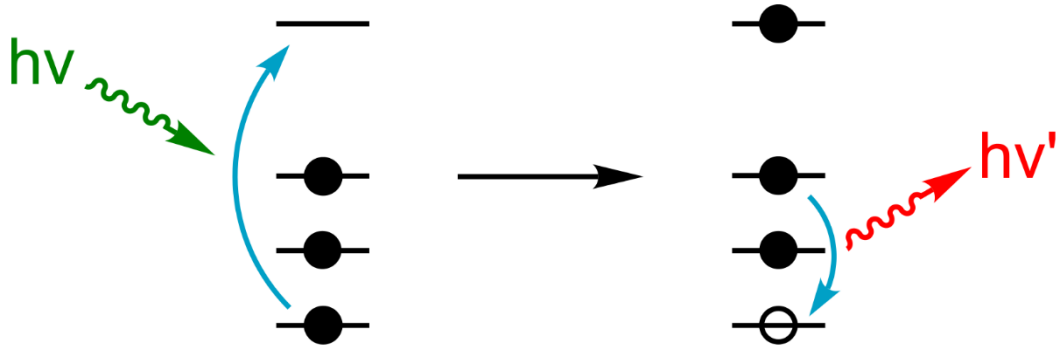

Fig 9. Physics of X-ray fluorescence in a schematic representation.

With X-rays as more powerful than electrons, XRF can detect elements from Sodium to theoretically, the end of the periodic table, and the rays can get deeper into the sample (ca. 1μm for SEM-EDS; ca. 10-100 μm for XRF) .Like SEM-EDX, the sampling of XRF require prepared plane surface for quantitative analysis. Depending on the machine used, sample should be in power form or polished in an epoxy resin (micro-XRF). Furthermore, XRF requires standards which have the same texture and density as the samples. Also there is limitation for glass analysis: quantitative analysis for elements lighter than aluminum and silicon are not recommended even with well-prepared samples with using standards.

XRF analysis is relatively inexpensive and very powerful in quantifying chemical elements in glass, and to identify glass sub-groups which may be linked to production sites. However, for provenance studies, XRF is sometimes not precise enough. Instrumental neutron activation analysis (INAA) or laser ablation inductively coupled plasma mass spectrometry (LA-ICP-MS) may be better suited for this purpose. [45]

4.2.2. Laser Ablation Inductively Coupled Plasma Mass Spectrometry (LA–ICP–MS)

One of the most recently developed analytical techniques in the field of archaeometry is a laser ablation sampling coupled to inductively coupled plasma – mass spectrometry (LA–ICP–MS). The general overview of the technique, explanation how does it work and what the main advantages are, as well as its methodology when applied to the glass materials will be given.

LA–ICP–MS is an extremely precise and sensitive technique, which is used to study a variety of archaeological materials, for example glasses, obsidians, bones, pottery, metals, written heritage etc. With a help of LA–ICP–MS is possible to detect and quantify elements even with concentration of 0,1 ppt. That is why this technique is the first choice when it comes to detecting of trace elements. In archaeometry, especially in glass studies, LA–ICP–MS is suitable for investigation of the provenance of the raw materials by use of trace element patterns to discriminate the provenance of the analyzed samples.

Laser Ablation Inductively Coupled Plasma Mass Spectrometer is a combination of three devices:

1. a laser that ablates a spot with a diameter from several dozens to several hundred of micrometers of the sample;
2. a plasma source which ionizes the ablated material;
3. a mass spectrometer which sorts the ions depending on their mass and charge.

Full representation of the LA–ICP–MS instrument can be seen on the (Fig)

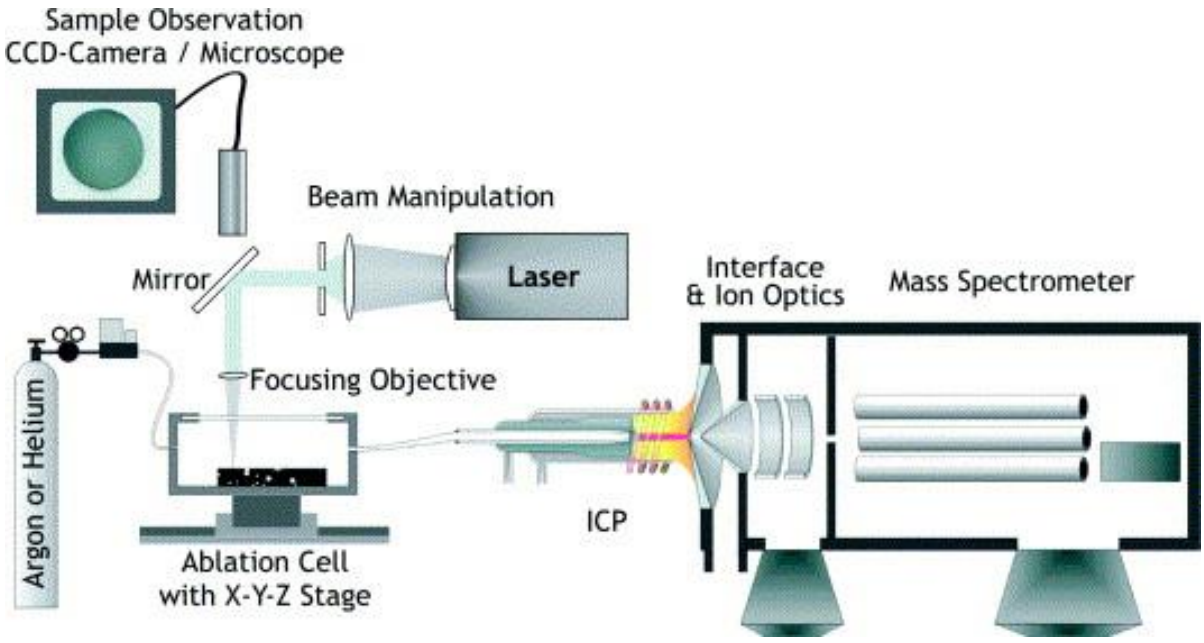

Fig..10. A schematic overview of LA-ICP-MS system (*Solid sample analysis using laser ablation inductively coupled plasma mass spectrometry)* [46]

The sample introduction begins from placing the sample inside a chamber, where a laser is focused on the 10-100 μm point on the surface of the sample and is about to be ablated. After ablation, material is then carried with He to ICP torch where it is atomized, ionized and carried to the interface.

Interface is needed due to differences in temperature and pressure – from 10000K and ambient pressure to room temperature and vacuum. Interface allows connecting ion source to mass analyzer. [47]Interface is composed by ion optics, main purpose of which is to separate the ions from particulates, photons and uncharged particles and to prevent entering of non-ions to mass analyzer. The mass analyzer then separates and quantifies the ions according to their mass-to-charge ratio (m/z). Mass analyzers can different, for example a quadrupole, a triple quadrupole, time-of-flight etc. After that the detector converts the ions into electrical pulses and the results of the analysis are presented in the form CPS or concentrations on the computer's monitor.

For the glass analysis silicon is often used as an internal standard.

One of the main advantages of LA-ICP-MS comparing to other mass-spectroscopy techniques is preforming a fast multi-element analysis with the lowest detection limits of elements, and absence of a sample preparation. LA-ICP-MS is micro-invasive technique, with the spot of an analysis almost invisible to a naked eye. Other important advantages of this technique are:

- spot analysis with high spatial resolution;
- depth profile studies;
- fast ;
- user friendly.

Even a very small piece of glass is enough to analyze and obtain reliable results. LA-ICP-MS is one of the few techniques precise enough to give the information about provenance of the glass. The main disadvantage of this technique is that its costliness.

5. Results

5.1. XRF results

The XRF analysis was carried out in a diagnostic laboratory for the Cultural Heritage objects “Ars Mensurae” under the supervision of Prof. Ridolfi. The XRF system used has a Molybdenum source of X-Rays, that is why the peak of Mo will be always present in resulting spectra. The XRF system has Silicon Drift Detector.

The data obtained was quite difficult to analyze, as a typical spectrum had peaks of Ar, Ca, Sc, Mn, Fe, Sr, Zr and Mo (from the X-Ray source), and these elements needed a careful revision in the spectrum, as their peaks can overlap, masking the real value of an element in a peak .For example, Kb of Ca has almost the same energies as Ka of Sc, and Kb of Mn – same energies with Ka Fe, and Fe Kb is similar to Co Ka, as well as Sr, Zr and Mo Ka and Kb energies have similar values, resulting “neighboring” elements to overlap in a spectrum. Thus, a thorough data treatment and recalculation of almost all the data obtained from 124 samples was needed.

All the recalculated values were put in a table for the convenience, as, of course, putting 124 spectra images in a results section would not be possible.

Regarding the results, apart from the mentioned typical elements, there are ones that appear often, but were not detected in each of the analyzed fragments, such as Co and K.

Such light elements as Na, Mg, Al, Si, P, S and Cl appeared in the spectra with very small count rates and in half of the cases it was not possible to even obtain a value of gross area of the peak. This is linked to detection limits of XRF system and even if a value from Si peak cannot be obtain, one keeps in mind that the material analyzed has 60-80% of Si, which is later confirmed by LA-ICP-MS.

Only several spectra did not show a presence of Mn, but mostly the count rates for Mn were similar to count rates of Fe. Mn and its contribution to this study which will be discussed in the next chapter.

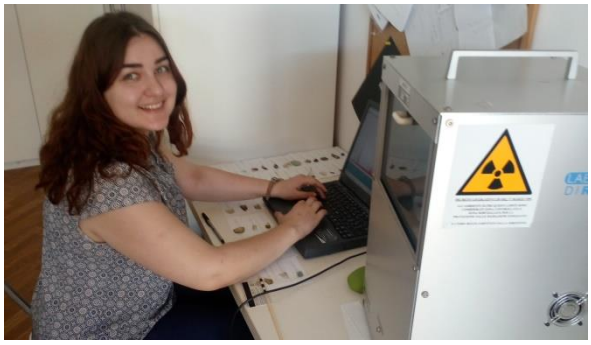

Fig..11 The author obtaining an XRF spectrum in the “Ars Mensurae” diagnostic lab

Table 2.Results of XRF analysis, measured in counts

	Na	Mg	Al	Si	P	S	Cl	Ar	K	Ca	Sc	Ti	V	Cr	Mn	Fe	Co	Ni	Cu	Zn	Ge	As	Sr	Zr	Mo
36073-001	1	10	3	10	6		11	65	15	111	17	14			564	540							230	104	117
36073-002	10	11	12					67	4	193	11	7		10	739	614		23	23				235	87	57
36073-003	1	26	4	5	10			63	13	128	14	3			678	467	68						241	132	75
36073-004	2	6	4	4				50	6	128	11				376	520	58		44	111		54	210	96	79
36073-005	8	7	11	15		75		3	3	149	9	11		20	822	713			37				257	143	102
36073-006	8	4	6	2				55	11	161	12	19			468	450	76						256	133	228
36073-007	7	7		3				68	10	107	2				208	132	28						143	152	160
36073-008		6	4	4				79	27	79					154	746	70						199	78	128
36073-009	13	6		5				52	16	81	14				320	377	36						241	136	99
36073-010	22	3	7	17				65	46	85		18	17			553	31		123	19		50	64	85	188
36073-011a	12		7	16				55	2	100	10				359	324	27						159	60	89
36073-011b	5	11	7	3				73	8	143	15				333	408	27					54	230	103	45
36073-012	10	3	6	4				39		132	12	19			557	589	53					64	329	62	95
36073-013	6	13	4	6				82		104	3				528	506	27						169	53	115
36073-014	8	2	21	2				61		122					450	552							336	79	86
36073-015	9	11	5	1	14			62	39	72	18					566	97		15				131	82	68
36073-016	3	11	11	5				73		78	17				255	493	90						157	62	163
36073-017	4	4		7				65		50	10					148	45						99	45	143
36073-018	4	12	6	3				72		122	22				357	154							93	77	159
36073-019	4	3	5	7				67		83	24				288	101	40						59	251	59
36073-020	7	9	8	16				56		144	9				706	625							313	152	92
36073-022	5	7	6	5				56		94	18				343	303	52						232	72	125
36073-023	6	6	2	10				55		40	6				149	438	37			37			99	252	55
36073-024	5	9		8				72		60					66	317	41						146	129	226
36073-025	4	12	1	11				57	14	76	12	7			115	485	25						235	187	95
36073-026	1	2	9					83	26	81					424	451	81						248	85	145
36073-027	7	16		8				52		163	25				338	223	64						223	94	227
36073-027a	2	6	7	6				39		67	16				207	137							104	146	149
36073-028	12	5		7				63	19	79	9				243	580	53						102	120	145
36073-029	10	2	21	5				71		151		19			10	1352	50						120	174	86
36073-030	7	9		8			15	70	16	104	11	26			457	391	56						165	159	68

Table 2.Results of XRF analysis, measured in counts (cont.)

	Na	Mg	Al	Si	P	S	Cl	Ar	K	Ca	Sc	Ti	V	Cr	Mn	Fe	Co	Ni	Cu	Zn	Ge	As	Sr	Zr	Mo
36073-031	4	4	10	15				65	2	114	14				386	489	9						281	147	87
36073-032	7		2	3				66	7	79	4				232	235			41				75	209	142
36073-033	19		4	6				78		115						163			11			67	188	371	107
36073-034	13		6	2				62	15	93	19				474	428	52	8	25				136	121	131
36073-035	4	17	1	3				57		86					220	251	31			34			126	136	82
36073-036	3		6	3				56	23	55	23				330	290	47			39			96	76	109
36073-037	4	2	5	3				70	39	61					357	407	28			17		93	56	70	58
36073-038	3	6	4	4				57	8	71	13				383	374	67		41	24			235	35	136
36073-039	4	5		4				67		141	23				478	467	88	15					121	325	71
36073-040	6		4	3				71		97	11				432	226	55						132	108	148
36073-041	8	5	3	4				34		91	16				587	543	57	12	45				321	67	155
36073-042	3	5		3				65	4	113	11				620	477	28	10					127	53	82
36073-043	4	6	8	3				51		82	17	10			261	202	70						171	90	67
36073-044	3		5					68	6	94		8			398	349	54						144	322	94
36073-045								60		106	9				410	433	43	8	21	36		41	222	257	118
36073-046							10	47	14	83					20	373	27		66				117		105
36073-047								47	22	99					180	363	19						242	104	108
36073-048								68		105	12	29			566	572	19						121	192	83
36073-049	3	16		2				60	12	77		17			134	620	10						203	121	204
36073-050								70	16	124	34				440	417	30						200	99	150
36073-051								69		114	19	29	20		719	540	27						127	146	109
36073-052								64	16	130	10	60			1239	1126		31	25			191	60	128	195
36073-053								77		115	12	14			486	378	66						275	116	124
36073-054								73		108	19				529	615	26						297	60	163
36073-055								68		111	14				486	407	86						179	49	102
36073-056	3	39		7				71	7	132					425	391	55						260		152
36073-057	6	6	12					72		59					399	483	29						169	298	133
36073-058	41			16			7	65	21	84	8				18	318	49						242	68	75
36073-059	10	12						67		99					289	142	17		41			52	100	82	187
36073-060	8	10	6	10	5			62	13	68					1501	1248	42		15	49		73	246	113	115

Table 2.Results of XRF analysis, measured in counts (cont.)

	Na	Mg	Al	Si	P	S	Cl	Ar	K	Ca	Sc	Ti	V	Cr	Mn	Fe	Co	Ni	Cu	Zn	Ge	As	Sr	Zr	Mo
36073-061	14	21						63	5	47					25	472	78		93				146	132	57
36073-062		25	11	7				53	37	69					132	579	75			43			194	130	69
36073-063	12	11	10	13				54		153					587	571	55						224	54	46
36073-064	21	6	5	8	15			48	5	100		86			5055	1769			67	86		122	75	92	79
36073-065	5	5		10				62	6	58					588	1102			71	38		125	99	112	144
36073-066	2	5	4	5				60		83	15				229	178	21						70	93	47
36073-067	6	3	4	4				75	14	78					319	445	14						189	45	207
36073-068	17		4	8				62		88	17				607	496	77	67					242	76	58
36073-069	21		10	5				59	5	79	17					487	65						242	90	46
36073-070	17		7	9				75	5	108	12				628	454	12						210	44	79
36073-071	3		3	4				53		90					366	443	65						201	72	113
36073-072	11	13	2	8				76	25	44		59		20	2464	1292			52			176	82	122	111
36073-073	4	6		5				51	19	164	19				336	500							264	177	73
36073-074	1	9	9					75		62	25	38			685	1108		15					189	72	127
36073-075		7	3	9				62	20	90	12	27			635	649	16		16	78		145	199	54	52
36073-076			14	4	8			63	4	158	13				351	462	62						182	69	78
36073-077	5	4	6					55	10	92	16	12			31	195							220	191	188
36073-078	1	13	15					58		90					284	171			23				275	316	315
36073-079	3		5	2				66	12	137	10	11			570	477	8						142	96	100
36073-080	4	12	7	9				76	13	124	5				595	397	97		41				185	167	85
36049-001		12						32		64	11	27			564	764	59						145	298	85
36049-002								50	21	72					62	273	28		15	40			138	92	46
36049-003	4	8		7				47	7	67	14				163	242	29	20	164				202	119	116
36049-004								61		62					230	165	13						112	181	108
36049-005			16					53		59					65	243	27	33	21			56	96	85	135
36049-006	9			5				64		54					605	438	20						156	258	123
36049-007	8		14					44		69		27			449	703							83	96	108
36049-008	14		2	5				76		85					311	267	33						96	60	80
36049-009				3				72		56	10	9			478	736							67	137	87
36049-010	5	5		3				58		56	10	9			478	736				25			200	69	93

Table 2.Results of XRF analysis, measured in counts (cont.)

	Na	Mg	Al	Si	P	S	Cl	Ar	K	Ca	Sc	Ti	V	Cr	Mn	Fe	Co	Ni	Cu	Zn	Ge	As	Sr	Zr	Mo
36062-001	14							66	17	99		34		7	586	799	60						97	71	71
36079-001	14		6	5				58	11	54		14			390	508	25						137	12	158
36079-002	4	4	5	5				58		117					463	316							199	46	91
36079-003	2	17		8				78	14	103					207	318	82		43			90	192	39	119
36079-004	6	7	7					51	8	81					359	536	75						273	210	243
36079-005		2						79	8	113	21				427	563	81		29			61	350	233	187
36079-006	5		4	12				55		141	29				654	797	36		38	64			279	132	49
36079-007	3	15						66	3	116					436	291	27						319	242	293
36098-001	14			4				77	14	82	5	7			72	739	24	29					349	224	253
36098-002	4		9	11				71		96	14				364	299	29						369	246	145
36098-003	2	7	4	4				67	26	84					80	292	72				29		146	76	89
36098-004	3		4	7				107	27	200	20				2090	1373	61		124	64		91	306	291	206
36098-005	12	16	13	2				52		91	6	4			254	311	38						120	113	200
36104-001	4	8		4				87	9	101	18					160	10						113	85	114
36104-002	7	9	7	8				70	6	91					56	147							219	250	247
36104-003	1	4		15				67	31	77						136	49						334	121	272
36104-004	9	13	4	3				65	22	68	10				26	375	42					179	116	85	118
36108-001	7	6	4	6				77	8	120	20				429	569	41						380	221	286
36108-002	2	1	12	4				77	4	61	14				374	308	36			25		41	270	241	196
36108-003	6	22	4	20				73		108	24				432	501	22	26	45	41		32	432	299	194
36108-004		6		7				52	15	71	13				163	144	32						193	163	155
36192-001	3	6	5	4				73	2	82	23				241	139		13					223	176	221
36072-001	5	15		19				65	22	108	7				52	198	42	20					273	325	391
36072-002	20		3	9				66	13	81	16				174	245	25		20				291	261	207
36072-003	3	8	11	8				67	17	97	11				572	611	27						413	366	308
36072-004	22		5	7				73	12	88		34			674	2058				61			303	305	248
36072-005	17		5					54	9	113	7				504	534	30	26					366	284	177
36072-006	12	6		11				62	10	78	29				499	521	51						401	259	248
36072-007	4	7	4	9				68	20	107	13				595	563	51	39	15				380	341	305
36072-008	3	5	17	8				30		81	7				5	64	22						105	76	78
36072-009	4		9	6				56	23	80						163	57					139	312	405	247

Table 2.Results of XRF analysis, measured in counts (cont.)

	Na	Mg	Al	Si	P	S	Cl	Ar	K	Ca	Sc	Ti	V	Cr	Mn	Fe	Co	Ni	Cu	Zn	Ge	As	Sr	Zr	Mo
36095-001	5	9	7	4				77	11	22					46	798	47		52	64			65	104	150
36095-002	6	4	11	6				65	19	111	11				522	479	35						305	279	181
36103-001	2	8	2	5				53	38	74		20			688	797	14						113	124	89
36103-002	5	15	2	10				80	1	77		5				251	43	11				81	244	141	354
36103-003	4	2	4					52	3	109	21	19			542	418	61		51				338	244	233

The names of fragments highlighted with a blue color in Table 2 were analyzed with both XRF and LA-ICP-MS.

The XRF results will be used in the study of (de)colorants, and it should give us an answer upon the deliberate usage of the such decolorizing agents as Mn.

5.2. LA-ICP-MS results

For the LA-ICP-MS analysis we had to significantly reduce the amount of fragments for the analysis, in order to still represent each layer, but to make the analysis in a one run. Fortunately, we were able to analyze 18 glass fragments. It was chosen to make 3 spots per each fragment, 85 μm in diameter each.

In this study BCR2G, a well-known and fully characterized basalt glass was used as a certified reference glass, as well as a standard reference material NIST 610 and NIST 612, commonly used in trace elements studies in glass as CRM.

The equipment used for the analysis are a Photon Machine G2 193 Excimer Laser Ablation system connected to the Thermo Fisher Scientific iCAPq quadrupole ICP-MS.

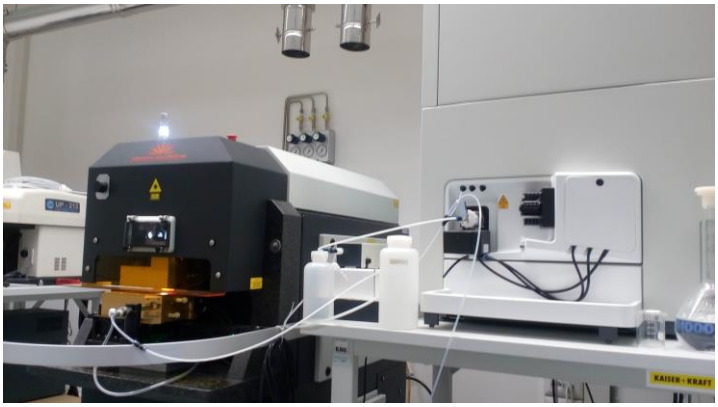

Table 3. LA-ICP-MS setup

Spot Size	85 μm
Laser Energy	10%
Shot count	600
Rep rate	8 Hz
Fluency rate	0.67 J/cm^2

Fig. The LA-ICP-MS system of the University of Perugia

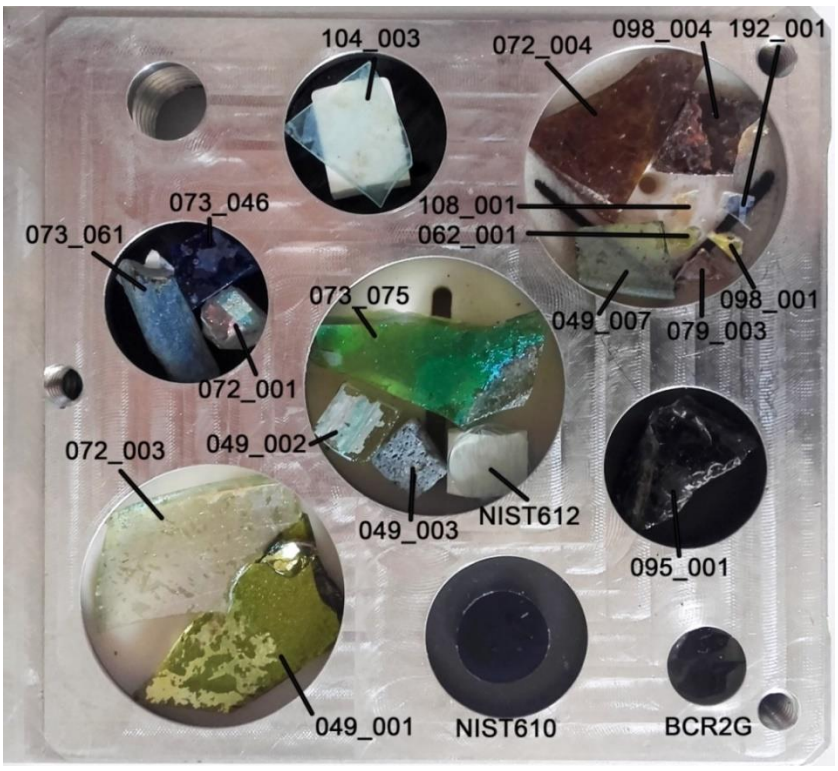

Fig. Glass fragments selected for LA-ICP-MS study

Table 4. Correspondence of names of fragments analyzed to spots in LA-ICP-MS analysis

Name of a fragment	Spot of the analysis
36192_001	10, 11,12
36108_001	52, 53, 54
36104_003	1, 2, 3
36098_001	13, 14, 15
36098_004	7,8,9
36095_001	25, 26, 27
36079_003	22, 23, 24
36073_046	46, 47, 48
36073_061	49, 50, 51
36073_075	40, 41, 42
36072_001	43, 44, 45
36072_003	31, 32, 33
36072_004	4, 5, 6
36062_001	16, 17, 18
36049_001	28, 29, 30
36049_002	34 35, 36
36049_003	37, 38, 39
36049_007	19, 20, 21

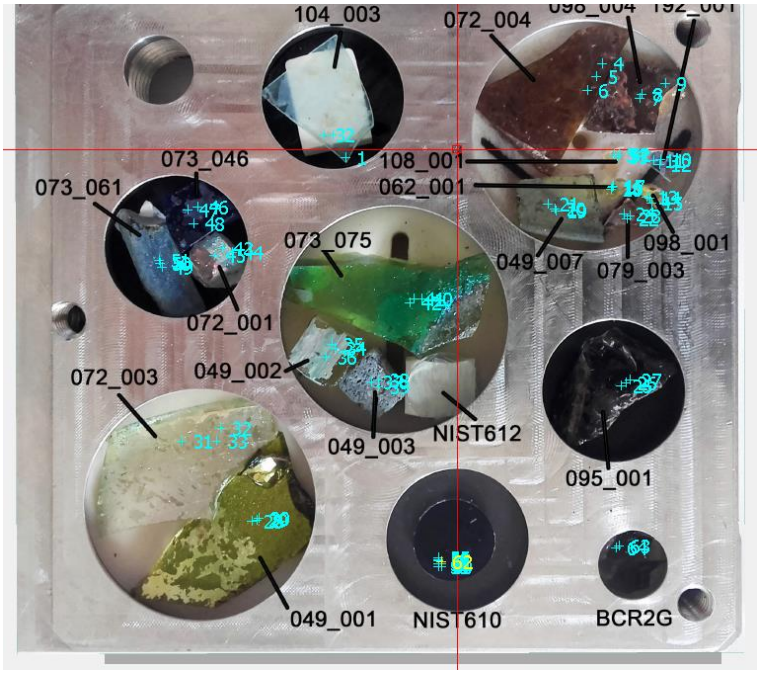

Fig. Glass fragments with the spots for analysis inside the Laser Ablation chamber

The LA-ICP-MS analysis helped us to acquire the wt% of Major elements of analysed glass fragments as shown in the Table 5.

Table 5. Major Elements measured by LA-ICP-MS instrument in wt, %

	SiO_2	Na_2O	MgO	Al_2O_3	P_2O_5	K_2O	CaO	TiO_2	MnO	FeO
S_1	70,4	15,1	0,6	3,1	0,1	0,9	9,2	0,1	0,0	0,4
S_2	70,7	14,9	0,6	3,1	0,1	0,9	9,2	0,1	0,0	0,4
S_3	70,5	15,1	0,6	3,1	0,1	0,9	9,1	0,1	0,0	0,3
S_4	66,1	16,6	1,3	3,4	0,2	0,5	6,0	0,7	1,7	3,3
S_5	66,3	16,7	1,3	3,4	0,1	0,5	5,9	0,7	1,7	3,2
S_6	66,1	16,9	1,3	3,3	0,1	0,5	5,9	0,7	1,7	3,2
S_7a	61,6	0,4	0,8	4,6	1,9	2,1	7,9	0,9	13,0	5,0
S_7b	79,0	0,2	0,6	10,1	0,2	1,7	4,7	0,3	0,2	2,6
S_8_a	60,5	0,3	0,6	6,1	1,1	1,7	6,8	0,9	16,3	3,8
S_8b	76,7	0,2	0,6	9,7	0,2	1,6	4,8	0,4	3,0	2,6
S_9a	56,9	0,4	0,8	5,7	4,5	2,3	12,2	0,6	10,6	4,6
S_9b	61,2	0,2	0,7	7,5	1,2	1,6	7,3	0,7	15,4	2,8
S_10	70,3	15,7	0,7	2,7	0,1	0,5	8,4	0,1	1,1	0,4
S_11	70,4	15,9	0,7	2,6	0,1	0,5	8,2	0,1	1,1	0,4
S_12	70,1	15,9	0,7	2,7	0,1	0,5	8,4	0,1	1,1	0,4
S_13	74,3	0,2	0,7	13,5	0,1	2,0	5,6	0,4	0,0	3,0
S_14	74,7	0,2	0,6	13,0	0,1	2,1	5,3	0,4	0,0	3,4
S_15	72,4	0,2	0,6	13,8	0,1	2,1	5,7	0,6	0,0	4,2
S_16	66,2	19,1	1,0	2,8	0,1	0,4	6,1	0,6	2,2	1,5
S_17	66,2	19,3	1,0	2,8	0,0	0,4	6,0	0,5	2,1	1,4
S_18	66,1	19,3	1,0	2,8	0,1	0,4	6,1	0,5	2,2	1,4
S_19	77,6	0,4	0,5	13,0	0,1	2,1	4,1	0,5	0,1	1,4

Table 5. Major Elements measured by LA-ICP-MS instrument in wt, % (cont.)

	SiO_2	Na_2O	MgO	Al_2O_3	P_2O_5	K_2O	CaO	TiO_2	MnO	FeO
S_20	75,0	0,5	0,6	14,3	0,1	2,3	5,0	0,6	0,1	1,4
S-21	73,0	0,6	0,6	14,9	0,1	2,6	5,9	0,6	0,1	1,4
S_22a	69,9	1,0	0,8	12,2	1,3	3,1	6,7	0,2	1,6	2,3
S_22b	66,5	16,3	1,2	3,2	0,2	1,0	8,2	0,2	1,9	1,1
S_23a	73,6	0,6	0,7	13,9	0,5	3,0	5,9	0,1	0,4	1,0
S_23b	66,7	15,9	1,2	3,8	0,2	1,1	8,1	0,2	1,6	1,0
S_24a	73,2	0,4	0,7	13,1	0,3	3,6	5,7	0,1	0,8	1,7
S_24b	66,6	16,9	1,2	3,1	0,2	1,0	7,9	0,2	1,7	1,0
S_25	75,3	4,2	0,0	13,1	0,0	5,0	0,7	0,1	0,1	1,4
S_26	75,0	4,2	0,0	13,1	0,0	5,1	0,8	0,1	0,1	1,4
S_27	75,0	4,1	0,0	13,3	0,0	5,1	0,7	0,1	0,1	1,4
S_28	64,5	21,5	1,0	2,7	0,0	0,3	5,7	0,6	2,0	1,4
S_29	64,3	21,5	1,1	2,7	0,0	0,3	5,7	0,6	2,0	1,4
S_30	64,3	21,5	1,1	2,7	0,0	0,3	5,7	0,6	2,0	1,4
S_31	66,3	17,1	1,2	2,8	0,2	0,9	8,5	0,2	1,7	1,0
S_32	65,7	17,2	1,2	2,8	0,2	0,9	8,8	0,2	1,8	1,1
S_33	64,9	17,2	1,2	2,9	0,3	0,9	9,2	0,2	1,8	1,2
S_34a	75,6	0,6	0,6	12,4	0,2	3,3	5,7	0,2	0,3	0,9
S_34b	69,2	17,9	0,7	2,6	0,1	0,7	6,7	0,1	0,7	0,7
S_35a	75,2	0,4	0,5	14,0	0,0	3,0	5,7	0,1	0,2	0,6
S_35b	69,5	17,4	0,7	3,0	0,1	0,6	7,0	0,1	0,6	0,6
S_36a	76,5	0,7	0,5	12,1	0,1	2,9	5,4	0,2	0,5	0,9
S_36b	69,7	17,7	0,8	2,5	0,1	0,6	6,7	0,1	0,7	0,6
S_37a	75,4	0,6	0,5	12,6	0,2	2,4	6,9	0,1	0,4	0,8
S_37b	72,3	13,1	0,7	3,4	0,1	1,0	7,1	0,1	1,0	0,7
S_38	60,7	0,4	6,7	9,5	0,1	1,1	14,0	0,9	0,3	6,0
S_39a	77,4	0,8	0,5	9,6	0,3	2,7	6,0	0,2	0,8	1,3
S_39b	70,5	13,8	0,7	3,5	0,2	1,0	7,3	0,1	1,3	0,9
S_40	66,6	19,0	1,0	2,6	0,1	0,5	6,8	0,4	1,7	1,2
S_41	66,4	19,3	1,0	2,6	0,1	0,5	6,7	0,4	1,7	1,1
S_42	66,5	19,3	1,0	2,5	0,1	0,5	6,7	0,4	1,7	1,1
S_43a	77,1	0,5	0,5	13,2	0,1	2,3	5,5	0,1	0,0	0,5
S_43b	70,9	18,8	0,4	2,3	0,1	0,7	5,7	0,1	0,2	0,3
S_44a	76,3	0,5	0,5	13,9	0,0	2,2	5,7	0,1	0,0	0,5
S_44b	70,8	19,2	0,5	2,0	0,1	0,5	5,8	0,1	0,2	0,3
S_45a	76,3	0,4	0,5	14,0	0,0	2,4	5,7	0,1	0,0	0,5
S_45b	72,8	15,3	0,5	3,6	0,1	0,8	5,8	0,1	0,2	0,4
S_46	69,9	18,4	0,6	2,1	0,1	0,6	6,3	0,1	0,2	1,0
S_47	69,8	18,9	0,6	2,0	0,1	0,5	6,3	0,1	0,1	0,9
S_48a	78,2	0,6	0,5	12,0	0,1	3,0	4,3	0,1	0,0	0,9
S_48b	70,4	18,6	0,6	2,0	0,0	0,5	6,3	0,1	0,1	0,7
S_49a	76,4	0,8	0,5	11,7	0,2	2,8	5,2	0,1	0,1	1,6
S_49b	69,7	19,1	0,7	2,2	0,1	0,5	5,7	0,1	0,1	1,0
S_50a	76,0	0,9	0,6	13,0	0,1	2,9	4,7	0,1	0,0	1,3
S_50b	69,3	19,4	0,7	2,2	0,1	0,5	5,8	0,1	0,0	1,1
S_51a	76,8	0,7	0,6	12,6	0,1	2,9	4,5	0,1	0,0	1,3
S_51b	69,6	19,2	0,7	2,1	0,1	0,5	5,8	0,1	0,1	1,1
S_52	64,6	19,3	1,1	2,4	0,1	0,6	9,1	0,2	1,4	1,0
S_53	64,7	19,3	1,1	2,4	0,1	0,6	9,1	0,2	1,4	0,9
S_54a	65,3	18,5	1,1	2,3	0,1	0,6	9,3	0,2	1,4	1,0
S_54b	65,1	19,2	1,1	2,4	0,1	0,6	8,9	0,2	1,3	0,9

Table 6. REE values in ppm obtained with the help of LA-ICP-MS

	La	Ce	Pr	Nd	Sm	Eu	Gd	Tb	Dy	Ho	Er	Tm	Yb	Lu
S_1	7,18	13,38	1,647	6,75	1,394	0,44	1,332	0,204	1,209	0,255	0,707	0,0906	0,665	0,0939
S_2	6,96	12,87	1,587	6,72	1,36	0,455	1,323	0,208	1,182	0,25	0,648	0,0942	0,599	0,0844
S_3	6,89	12,78	1,571	6,56	1,337	0,425	1,31	0,1985	1,193	0,257	0,662	0,091	0,633	0,0889
S_4	17,55	23,27	3,869	16,14	3,32	0,866	3,32	0,496	2,896	0,627	1,685	0,253	1,622	0,26
S_5	17,42	22,34	3,811	15,65	3,36	0,851	3,26	0,505	2,938	0,623	1,665	0,253	1,602	0,263
S_6	17,21	22,29	3,823	15,55	3,35	0,846	3,21	0,497	2,857	0,599	1,62	0,238	1,653	0,256
S_7a	79	130	20,1	71	14,8	5,2	12,3	1,93	9,7	2,01	5,2	0,72	6,3	0,93
S_7b	8	25,6	2,65	8,8	1,6	0,53	1,78	0,301	1,79	0,363	1,05	0,14	1,14	0,17
S_8_a	87	124	19,1	75	15,1	4,7	13,7	1,93	10,7	2,22	5,5	0,77	4,8	0,77
S_8b	13,9	39,4	3,29	12,4	2,98	0,75	2,54	0,377	2,33	0,481	1,42	0,203	1,56	0,204
S_9a	79	98	16,4	66	12,2	4,25	9,7	1,45	8	1,58	3,96	0,59	4,9	0,77
S_9b	69	131	14,4	55,2	10,2	3,04	8,9	1,32	7,49	1,51	4,14	0,586	4,04	0,593
S_10	7,24	12,97	1,636	6,89	1,363	0,438	1,417	0,203	1,233	0,251	0,675	0,1059	0,598	0,0902
S_11	5,24	9,48	1,179	4,96	1,017	0,311	0,997	0,147	0,876	0,1865	0,489	0,0647	0,446	0,067
S_12	5,85	10,34	1,301	5,43	1,161	0,353	1,064	0,1714	1,013	0,211	0,56	0,08	0,526	0,0795
S_13	6,38	35,4	1,97	8,05	1,62	0,504	1,63	0,264	1,72	0,352	0,92	0,119	0,71	0,124
S_14	9,04	41	2,81	11,37	2,54	0,649	2,09	0,341	2,25	0,452	1,12	0,171	1,12	0,154
S_15	16,6	54,7	5,25	20,2	4,38	1,099	3,75	0,611	3,76	0,754	1,93	0,314	2,01	0,257
S_16	13,8	20,22	2,952	12,51	2,63	0,675	2,51	0,382	2,375	0,486	1,362	0,21	1,42	0,22
S_17	13,7	20,04	2,917	11,94	2,56	0,668	2,44	0,379	2,249	0,488	1,35	0,211	1,375	0,215
S_18	13,35	19,46	2,855	11,92	2,473	0,673	2,41	0,381	2,204	0,479	1,299	0,195	1,326	0,224
S_19	2,17	3,24	0,657	2,76	0,57	0,119	0,18	0,083	0,29	0,028	0,076	0,0053	0,074	
S_20	2,99	3,78	0,94	2,96	0,61	0,166	0,35	0,078	0,36	0,056	0,121	0,018	0,011	0,0107
S-21	2,96	4,1	0,91	3,26	0,6	0,171	0,42	0,075	0,398	0,06	0,184	0,0227	0,184	0,0247
S_22a	8,5	41,1	2,64	6,7	1,8	0,391	0,64	0,086	0,46	0,089	0,29	0,069	0,173	0,027
S_22b	13,54	26,7	2,68	11,04	2,13	0,59	1,96	0,272	1,748	0,371	0,976	0,144	0,947	0,143
S_23a	2,97	16,5	1,6	3,28	0,6	0,243	0,35	0,059	0,34	0,06	0,127	0,038	0,062	0,021
S_23b	11,5	22,4	2,45	9,89	1,87	0,498	1,89	0,244	1,46	0,322	0,827	0,132	0,83	0,124
S_24a	12	11,3	0,87	2,5	0,35	0,21	0,75	0,034	0,16	0,027	0,086	0,0133	0,062	0,018
S_24b	11,31	19,92	2,38	9,52	2	0,473	1,87	0,273	1,6	0,332	0,836	0,121	0,915	0,143
S_25	50,2	95,6	9,79	34,17	6,93	0,121	5,98	0,951	5,73	1,227	3,47	0,546	3,87	0,595
S_26	49	93,3	9,5	33,27	6,92	0,114	5,94	0,939	5,56	1,193	3,4	0,546	3,79	0,576
S_27	54,1	102,5	10,43	37,12	7,66	0,125	6,43	1,052	6,25	1,295	3,7	0,597	4,33	0,645
S_28	10,51	19,54	2,42	9,82	2,12	0,555	1,954	0,302	1,813	0,402	1,112	0,1771	1,196	0,192
S_29	11,75	21,42	2,649	11,03	2,27	0,658	2,12	0,345	2,017	0,451	1,229	0,187	1,348	0,212
S_30	10,72	19,48	2,357	9,79	2,064	0,551	1,966	0,299	1,852	0,393	1,108	0,1647	1,153	0,198
S_31	10,52	18,65	2,32	9,27	1,822	0,548	1,704	0,269	1,541	0,333	0,894	0,1355	0,903	0,1402
S_32	10,67	21,5	2,39	9,62	1,97	0,55	1,83	0,28	1,558	0,33	0,889	0,132	0,914	0,1319
S_33	12,61	25,1	2,71	10,26	2,13	0,558	1,802	0,298	1,633	0,358	0,915	0,1427	0,964	0,145
S_34a	3,4	18,3	0,64	2,03	0,53	0,168	0,37	0,042	0,164	0,04	0,102	0,02	0,122	0,0179
S_34b	6,81	13,9	1,583	6,3	1,3	0,323	1,19	0,174	1,091	0,222	0,604	0,091	0,527	0,089
S_35a	2,5	5,7	0,54	1,19	0,252	0,122	0,279	0,043	0,181	0,037	0,069	0,0123	0,093	0,0122

Table 6. REE values in ppm obtained with the help of LA-ICP-MS (cont.)

	La	Ce	Pr	Nd	Sm	Eu	Gd	Tb	Dy	Ho	Er	Tm	Yb	Lu
S_35b	6,68	11,91	1,481	6,15	1,23	0,338	1,22	0,181	1,032	0,22	0,579	0,078	0,566	0,082
S_36a	3,3	10,5	0,93	2,2	0,42	0,182	0,26	0,045	0,194	0,042	0,08	0,03	0,104	0,0169
S_36b	6,71	11,56	1,442	6,05	1,23	0,358	1,17	0,188	1,062	0,227	0,603	0,086	0,518	0,087
S_37a	3,38	9,7	1,15	2,44	0,6	0,195	0,27	0,056	0,33	0,072	0,133	0,0303	0,157	0,0187
S_37b	6,24	11,4	1,38	5,81	1,22	0,391	1	0,162	0,91	0,192	0,513	0,068	0,467	0,075
S_38	29,8	80,8	11,6	56,5	12,89	2,71	10,52	1,211	5,41	0,852	1,7	0,224	1,36	0,243
S_39a	4,64	21,5	1,51	4,2	0,76	0,264	0,48	0,087	0,298	0,072	0,156	0,035	0,214	0,032
S_39b	8,26	19,4	1,96	7,14	1,35	0,432	1,33	0,177	1,02	0,211	0,612	0,076	0,602	0,08
S_40	11,37	18,89	2,55	10,04	1,998	0,554	1,874	0,309	1,806	0,373	1,038	0,1513	1,056	0,174
S_41	10,32	16,75	2,219	9,36	1,865	0,502	1,8	0,279	1,647	0,354	0,952	0,1409	0,978	0,153
S_42	11,2	18,16	2,411	10,05	2,056	0,552	1,942	0,316	1,764	0,395	1,049	0,166	1,109	0,1641
S_43a	1,13	4,7	0,81	1,15	0,33	0,095	0,1	0,038	0,137	0,039	0,094	0,018	0,165	0,024
S_43b	5,6	9,53	1,245	5,15	1,1	0,3	1,03	0,144	0,9	0,15	0,529	0,066	0,5	0,094
S_44a	0,7	3,38	0,183	0,87	0,159	0,066	0,182	0,0291	0,162	0,033	0,088	0,018	0,145	0,0161
S_44b	6,39	10,63	1,378	5,75	1,18	0,362	1,06	0,173	1,03	0,199	0,53	0,082	0,518	0,071
S_45a	1,18	3	0,178	0,56	0,128	0,061	0,118	0,0156	0,088	0,024	0,06	0,0156	0,074	0,0036
S_45b	5,11	8,8	1,05	4,87	0,94	0,279	0,87	0,121	0,86	0,169	0,392	0,066	0,41	0,057
S_46	6,63	12,12	1,517	6,02	1,245	0,34	1,158	0,1664	1,011	0,204	0,551	0,0815	0,55	0,0836
S_47	6,33	11	1,361	5,52	1,132	0,339	1,078	0,161	0,983	0,199	0,565	0,0845	0,521	0,0789
S_48a	1,09	2,8	0,19	0,33	0,12	0,057	0,068	0,0071	0,098	0,019	0,042	0,014	0,047	0,0086
S_48b	5,24	8,88	1,173	4,71	0,939	0,271	0,803	0,137	0,863	0,178	0,466	0,0691	0,46	0,0612
S_49a	3,7	6,4	0,81	2,6	0,76	0,24	0,54	0,34	0,55	0,07	0,21	0,033	0,25	0,11
S_49b	7,04	12,62	1,559	6,54	1,284	0,37	1,208	0,188	1,052	0,224	0,617	0,091	0,594	0,09
S_50a	1,11	1,81	0,312	1,19	0,257	0,086	0,171	0,0202	0,207	0,041	0,11	0,0131	0,092	0,018
S_50b	6,74	11,99	1,454	6,03	1,21	0,335	1,149	0,173	1,138	0,223	0,588	0,0934	0,603	0,0858
S_51a	0,97	1,31	0,286	1,15	0,263	0,059	0,184	0,041	0,168	0,0366	0,074	0,0138	0,091	0,0183
S_51b	6,16	11,07	1,341	5,4	1,032	0,321	1,028	0,1516	0,898	0,19	0,512	0,073	0,488	0,0798
S_52	9,37	14,99	1,996	8,28	1,656	0,445	1,703	0,239	1,448	0,307	0,818	0,1213	0,791	0,1245
S_53	9,39	14,63	1,999	8,28	1,658	0,456	1,605	0,255	1,507	0,306	0,822	0,1239	0,796	0,1236
S_54a	8,95	14,9	2,02	8,1	1,44	0,71	1,48	0,221	1,34	0,27	0,672	0,095	0,64	0,106
S_54b	10,75	16,66	2,353	9,78	1,92	0,508	1,87	0,287	1,76	0,353	0,965	0,132	0,903	0,137

These REE values are important for the provenance analysis. In order to acquire an REE profile of the glass fragment, the values should be normalized by the REE amounts of a mineral chondrite, which means to divide values of fragments by the chondrite ones. This diagram will be shown and discussed in the next chapter.

Table 7. Trace elements values in ppm obtained with the help of LA-ICP-MS.

	Li	Be	B	Sc	V	Cr	Co	Ni	Cu	Zn	Ga	As	Rb
049_001	5,06	0,39	210,37	15,46	60,57	68,70	12,48	16,57	41,64	28,66	3,77	4,24	4,92
049_002	4,33	0,49	144,63	11,02	19,29	13,50	7,81	8,63	545,33	30,30	2,83	20,04	15,50
049_003	4,44	2,04	70,07	36,09	68,60	101,00	13,79	36,37	1282,33	28,73	7,00	11,27	45,63
049_007		4,13	7,60	14,34	29,30	79,07	0,93	1,41	19,07	7,25	6,32	18,67	108,63
062_001	4,54	0,41	163,63	17,90	53,90	68,00	13,01	21,64	47,77	20,39	3,85	4,08	5,45
072_001	3,55	0,69	220,27	11,20	9,32	9,87	2,38	4,21	22,33	19,60	3,18	19,47	16,30
072_003	13,55	0,71	202,83	14,36	44,60	22,67	11,40	25,50	128,03	51,37	4,74	8,10	27,40
072_004	5,76	0,67	173,83	18,95	95,20	78,50	13,52	42,06	78,70	53,93	4,59	17,09	9,37
073_046	4,68	0,26	196,43	10,90	13,40	10,35	182,33	11,43	1225,00	66,30	3,38	34,48	8,71
073_061	4,78	0,30	223,30	11,41	12,11	14,61	170,77	8,37	1416,00	43,37	3,64	32,03	7,58
073_075	5,85	0,47	195,87	13,81	38,53	45,23	9,95	17,09	64,67	34,50	3,55	5,52	11,77
079_003	12,54	0,65	148,27	15,11	41,63	21,60	13,68	24,03	236,50	51,57	4,31	9,32	27,80
095_001	78,40	6,84	186,27	12,08	1,46	0,51	0,37	0,28	7,21	54,00	15,41	17,54	282,27
098_001		1,71	2,96	21,77	19,70	68,70	0,17		62,33	30,93	9,56	22,07	103,77
098_004	1,65	1,67	5,57	21,49	123,73	37,63	39,13	67,00	840,00	391,67	10,92	27,50	87,13
104_003	3,38	0,35	58,03	16,70	8,04	13,01	1,38	3,91	18,49	9,11	3,16	2,16	14,24
108_001	7,82	0,44	186,63	11,57	32,71	16,72	9,26	13,62	98,57	26,56	2,96	5,88	14,24
192_001	2,97	0,28	82,23	13,12	11,26	14,13	2,75	8,56	13,46	12,58	2,44	2,30	6,83

Table 7. Trace elements values in ppm obtained with the help of LA-ICP-MS (cont.)

	Sr	Y	Zr	Nb	Sn	Sb	Cs	Ba	Hf	Ta	Pb	Th	U
049_001	507,37	11,14	305,87	6,13	1,70	1,60	0,07	861,33	7,47	0,46	14,85	2,54	2,15
049_002	451,00	6,29	57,10	1,95	36,33	1873,33	0,41	269,00	1,50	0,14	366,00	1,23	0,93
049_003	474,67	10,79	220,77	2,97	37,60	459,33	1,12	329,00	8,24	0,32	196,00	3,82	0,87
049_007	404,00	1,14	336,67	7,95	2,33	1,61	1,41	543,00	8,42	0,88	50,33	3,06	0,31
062_001	540,67	13,07	272,03	5,66	0,64	0,28	0,06	277,70	6,60	0,42	9,79	2,40	1,42
072_001	417,00	5,34	50,13	1,48	5,40	4116,67	0,28	196,10	1,31	0,13	95,20	0,99	0,85
072_003	904,00	9,25	95,43	3,67	18,61	157,10	1,29	495,33	2,43	0,24	326,00	1,99	1,95
072_004	489,23	16,49	320,03	6,90	2,11	0,84	0,24	396,53	7,74	0,50	89,13	2,81	1,64
073_046	449,13	5,67	44,43	1,59	55,87	3396,67	0,18	165,63	1,19	0,11	125,80	0,95	1,09
073_061	413,33	5,89	67,57	2,14	159,30	3827,00	0,11	164,53	1,75	0,15	200,40	1,18	1,12
073_075	573,63	10,27	191,83	4,30	6,92	40,86	0,26	379,57	4,74	0,30	276,00	2,05	1,49
079_003	834,67	9,45	117,37	3,67	19,20	266,33	0,94	455,67	3,16	0,27	309,67	2,58	1,40
095_001	16,26	36,45	152,10	28,42	5,79	0,90	14,66	16,73	5,78	2,16	31,97	45,43	14,15
098_001	456,53	10,07	419,67	8,26	2,88	4,25	1,42	764,67	11,22	0,90	43,90	7,10	0,39
098_004	432,33	20,57	345,00	9,10	107,17	385,33	1,66	2037,67	9,14	0,73	1508,00	5,29	2,26
104_003	499,43	7,55	36,88	1,34	1,24	2,39	0,15	253,73	0,97	0,10	25,53	0,84	0,61
108_001	804,33	9,18	89,17	2,73	21,07	187,57	0,22	394,37	2,27	0,20	348,60	1,63	1,44
192_001	422,40	6,47	36,39	1,23	0,77	4,55	0,06	243,60	0,94	0,09	10,79	0,75	0,72

6. Discussion

The data obtained from XRF and LA-ICP-MS will allow us to determine the type of glass of the fragments. For the Roman glass of that time it is expected to confirm that all the fragments belong to the natron soda-lime glass. However, if there is an intrusion fragment from a later period, it would be seen on ternary diagram, because there is a change of raw materials used for a glass production. In later periods of history, after The Fall of Western Roman Empire, natron was substituted by plant ash probably by several reasons, such as reduced or absent natron supplies from the shores of Egypt, a wish to create an easier and cheaper glass production technology and so on. Soda was later replaced by forest plant ash. However, mixed alkali glasses were known since the Bronze Age. [48]

A ternary diagram is a 2D plot with 3 variables that sum up to some constant. It is displayed as an equilateral triangle with its vertices corresponding to the maximum amount of a chosen element, or a compound in our case.

The plotted relation of amounts of Na_2O, CaO and sum of MgO with K_2O from the Table 8 can show to researchers the type of glass fragments are made of.

Table 8.Major elements for each fragment in wt%

	SiO_2	Na_2O	MgO	Al_2O_3	P_2O_5	K_2O	CaO	TiO_2	MnO	MgO+ K_2O
049_001	64,4	21,5	1,1	2,7	0,0	0,3	5,7	0,6	2,0	1,4
049_002	69,5	17,7	0,7	2,7	0,1	0,7	6,8	0,1	0,6	1,4
049_003	67,8	9,1	2,7	5,5	0,1	1,0	9,5	0,4	0,9	3,7
049_007	75,2	0,5	0,6	14,0	0,1	2,3	5,0	0,6	0,1	2,9
062_001	66,1	19,2	1,0	2,8	0,1	0,4	6,1	0,5	2,2	1,4
072_001	71,5	17,8	0,5	2,7	0,1	0,7	5,8	0,1	0,2	1,1
072_003	65,6	17,2	1,2	2,8	0,2	0,9	8,8	0,2	1,8	2,1
072_004	66,2	16,7	1,3	3,4	0,1	0,5	5,9	0,7	1,7	1,8
073_046	70,1	18,6	0,6	2,0	0,1	0,5	6,3	0,1	0,1	1,1
073_061	69,5	19,2	0,7	2,2	0,1	0,5	5,8	0,1	0,1	1,2
073_075	66,5	19,2	1,0	2,6	0,1	0,5	6,7	0,4	1,7	1,5
079_003	66,6	16,4	1,2	3,4	0,2	1,0	8,1	0,2	1,7	2,2
095_001	75,1	4,1	0,0	13,2	0,0	5,1	0,7	0,1	0,1	5,1
098_001	73,8	0,2	0,6	13,5	0,1	2,1	5,5	0,4	0,0	2,7
098_004	72,3	0,2	0,7	9,1	0,5	1,6	5,6	0,5	6,2	2,3
104_003	70,5	15,0	0,6	3,1	0,1	0,9	9,2	0,1	0,0	1,5
108_001	64,8	19,3	1,1	2,4	0,1	0,6	9,0	0,2	1,4	1,7
192_001	70,3	15,9	0,7	2,7	0,1	0,5	8,3	0,1	1,1	1,2

The following Fig.12 is a ternary diagram of major elements of glass fragments which was expected to confirm that all of the fragments belong to a soda-lime glass, however it seems not to be the case.

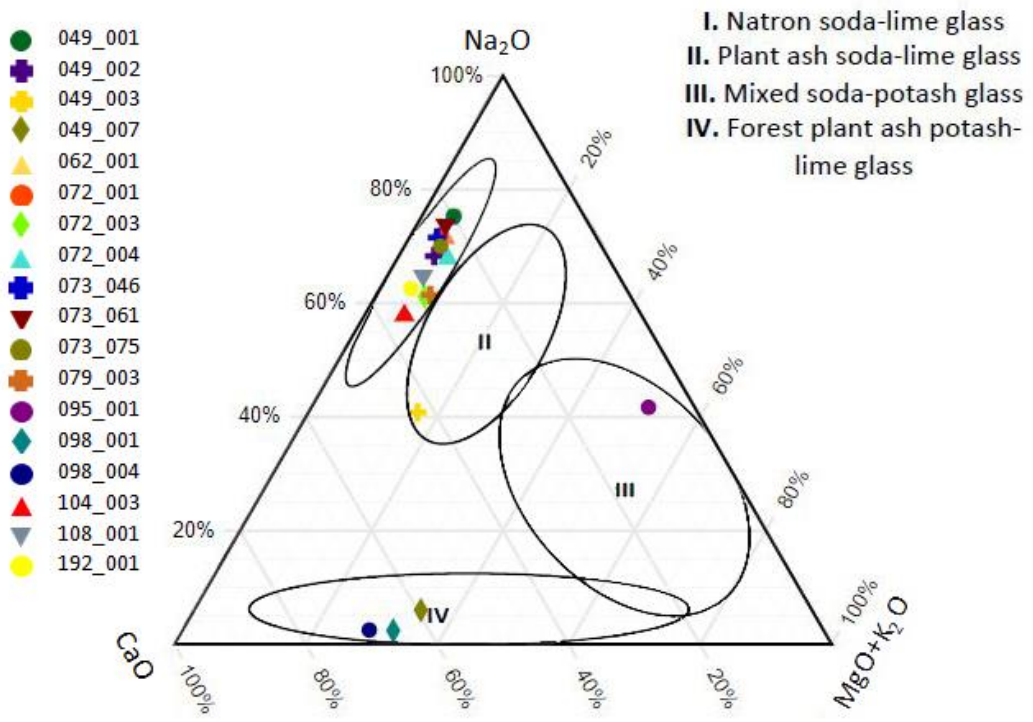

Fig.12. Ternary plot of major elements of glass fragments – Na_2O, CaO and sum of MgO with K_2O

Surprisingly, the major elements values obtained with the help of LA-ICP-MS, were able to fit into all four types of historical glass. During Imperial period and two centuries after the fall of Western Roman Empire natron glass is the type of glass that is described in literature sources, other types of glasses are believed to appear later, and there are archaeological evidences confirming that. Obtaining such a pattern on a ternary plot could be explained, without an assumption that Romans have found a new breakthrough technology of glass making without natron in 6^{th} - 7^{th} century AD. For the first explanation, one might find this periodic table with the elements used in glass production attributed to their sources (Fig 13) quite useful.

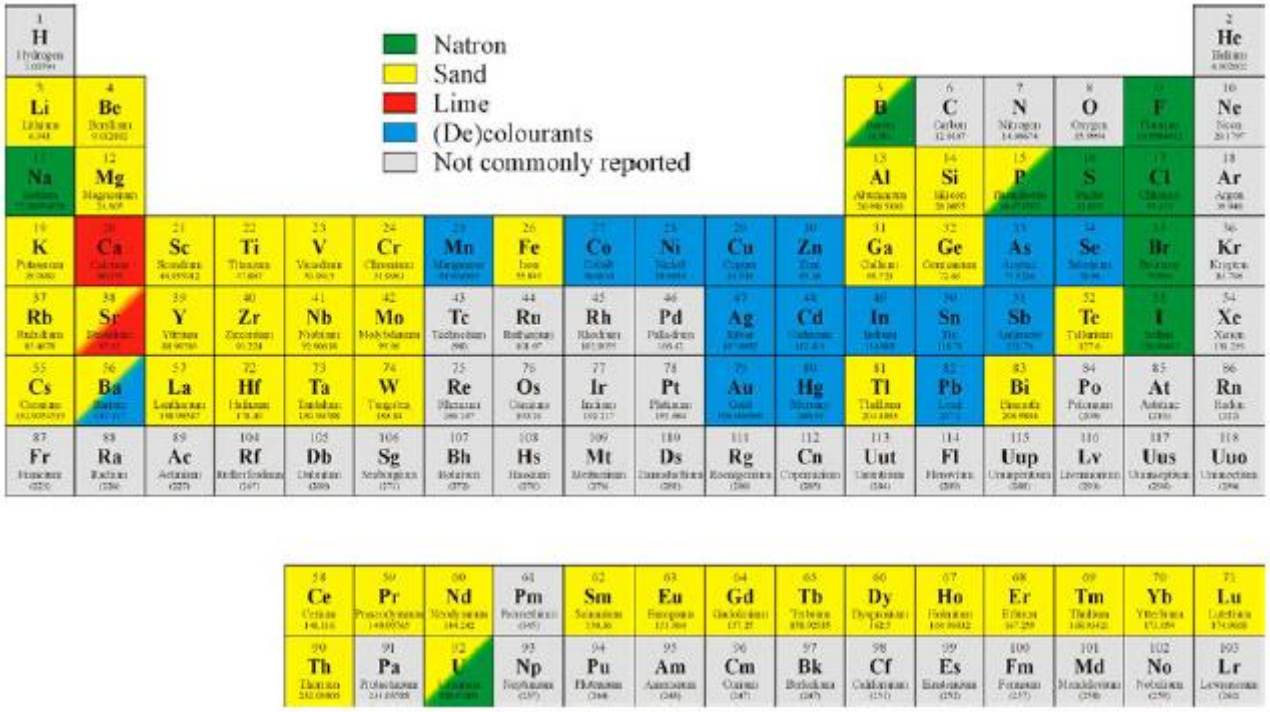

Fig.13 Periodic table with indication of the most likely sources of the elements in Roman natron glass.[14]

As it can be seen, the only possible source of sodium in a resulting glass is natron, and calcium is introduced in the glass batch with lime. Potash and magnesium derive from the sand.

It is possible, that these relatively high levels of K and Mg oxides could be explained if the sand for a glass production had inclusions of K and Mg-rich minerals.

As for the extremely low concentrations of sodium (less than 1%), the author hypothesizes that it could happen because of the thicker altered layer of glass, than it was expected. The approximate depth of the laser of LA-ICP-MS system penetration of the sample under the analysis parameters is 100-200μm, thus the altered layer depth should be higher than these values. Fragments 098_004 and 098_001 are indeed having an altered layer seen with a naked eye, nevertheless they were analysed as the only representatives of the layer that fit the dimensions required for LA-ICP-MS. These two fragments have similar amounts of CaO and MgO + K_2O compared to the majority of glasses that fit into the category of Roman natron glass.

The creation of sodium depleted layer in soda-lime glasses disposed to air is reported in the literature, however an accelerated (540min) creation of 5μm depletion layer requires a high direct voltage application.[49] Thus, it is quite possible for a 1,500 years old glass which was exposed to weathering, erosion and long-time burial to have a sodium depleted layer as well.

However in order to prove this theory a deeper and more expensive research, for example a study of Sr isotopes of this glass collection and comparing their values to already existing ones, should be performed.

After the data thorough analysis, a brief archaeometric characterization of analysed glass fragments could be made.

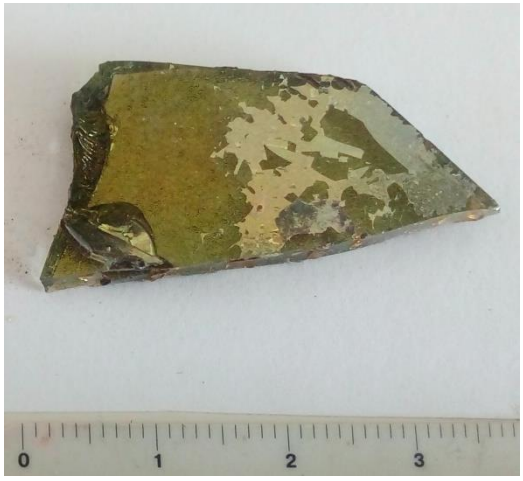

Fragment 36049_001

Object: a body part of a vessel
Type of glass: Natron soda-lime glass
Colorants and decolorants: High amounts of Fe (764 counts) detected by XRF is what producing the colour of a fragment with Fe^{2+} ions causing the yellow hue and Fe^{3+} - the green one. Besides, wt% (Mn) equals to 2%, which indicates it as a deliberate addition to the glass batch.
Evidences of recycling: Probably no, as the ppm levels of Pb and Sb are lower than 100, and Mn might be added for the (de)colorizing purpouses.
Other: Elevated levels of Ba, which could was probably introduced together with Mn in the mixture of pyrolusite MnO_2 and psilomelane. $(Ba,H_2O)_2Mn_5O_{10}$.

Fragment 36049_002

Object: a tesserae

Type of glass: Natron soda-lime glass

Colorants and decolorants: Very light aqua tint introduced with the small amounts of Fe and Cu, while Mn presence does not seem to be intentional. The elevated levels of antimony (1873 ppm) indicate an intentional decoloring.

Evidences of recycling: Lead amount of 366 ppm with the tesserae being almost colouress due to a big amount of Sb might indicate glass recycling.

Fragment 36049_003

Object: a tessera

Type of glass: Natron soda-lime glass or plants ash soda-lime glass.

Colorants and decolorants: Blue tint is caused by intentional addition of Cu (1282ppm).

Evidences of recycling: Lead and antimony amounts indicate glass recycling.

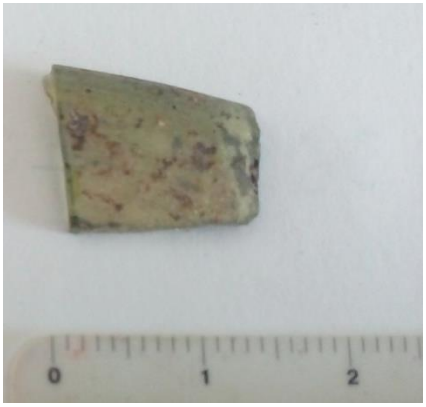

Fragment 36049_007

Object: a rim

Type of glass: Probably natron soda-lime glass

Colorants and decolorants: Light green tint is caused by iron (700 counts).

Evidences of recycling: None
Other: a big depletion in sodium amount on the glass surface.

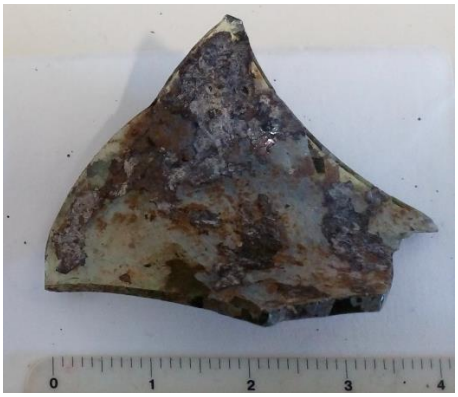

Fragment 36062_001

Object: a part of a neck of a glass vessel

Type of glass: Natron soda-lime glass

Colorants and decolorants: Green hue is caused by Fe (799 counts). Manganese amount exceeds 2%, thus was added in purpose.

Evidences of recycling: None

Fragment 36072_001

Object: a tessera

Type of glass: Natron soda-lime glass

Colorants and decolorants: The amount of 4116 ppm of antimony was added to the glass batch to ensure that the resulting glass will not have any hue.

Evidences of recycling: None

Fragment 36072_003

Object: a rim

Type of glass: Natron soda-lime glass

Colorants and decolorants: Fe causing the light aqua hue and a deliberate addition of Mn to decolorize the glass..

Evidences of recycling: Pb in the amount of326 ppm.

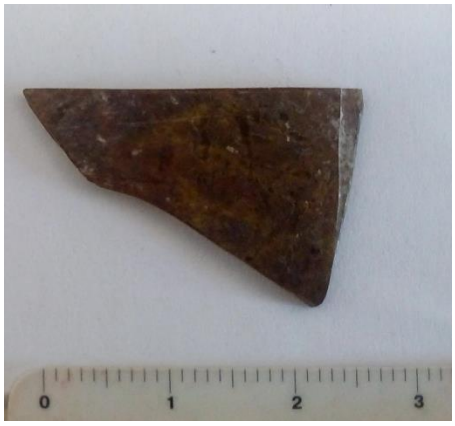

Fragment 36072_004

Object: a rim

Type of glass: Natron soda-lime glass

Colorants and decolorants: Vast amounts of Fe causing the yellow-brown color of the glass. A deliberate addition of Mn probably resulted in more deep brown colour.

Evidences of recycling: None

Fragment 36073_046

Object: a tessera

Type of glass: Natron soda-lime glass

Colorants and decolorants: Cu in quantity of 1225ppm as well as 182 ppm of Co causing deep blue colour to appear.

Opacifier : Antimony has been found in the amount of 3396pm, probably in order to remove any unnecessary tints and create an opaque tessera.

Evidences of recycling: None

Fragment 36073_061

Object: a part of the handle, coming from the burial

Type of glass: Natron soda-lime glass

Colorants and decolorants: Cu in aquantity of 1416,00ppm as well as 170 ppm of Co creating another the striking blue colour to appear.

Opacifier : Sb in quantities of 3827 ppm, that served mostly for opacifying the glass.

Evidences of recycling:Elevated levels of lead (200ppm)

Fragment 36073_075

Object: body fragment of a vessel

Type of glass: Natron soda-lime glass

Colorants and decolorants:. XRF shows elevated values of Fe (649 counts) and Mn (635 counts), thus only Fe ions causing the strong green-aqua tint.

Mn 1,7 % indicates deliberate addition.

Opacifier : No

Evidences of recycling: None

Fragment 36079_003

Object: base fragment

Type of glass: Natron soda-lime glass

Colorants and decolorants: Light blue colour was achieved with Cu in a quantity of 236,5ppm as well as 13,7 ppm of Co slightly elevated amounts. Co and Cu were also detected by XRF. Possible use of antimony as a decolorant.

Opacifier : Sb in quantities of 266 ppm made glass more opaque.

Evidences of recycling: 309ppm of Pb indicates recycling

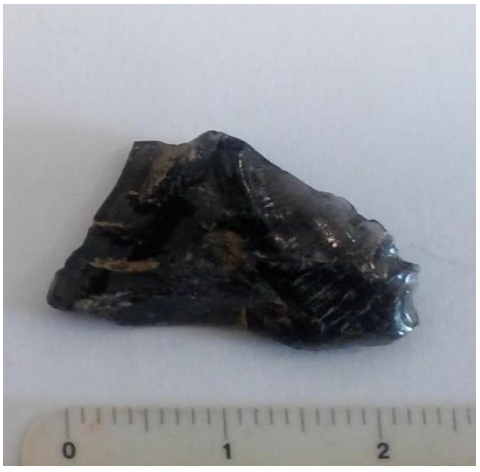

Fragment 36095_001

Object: probably a fragment of a wall of a vessel

Type of glass: Probably mixed-alkali glass

Colorants and decolorants: According to the data obtained, only Fe (739 counts) with no decolorants used was able to produce such a dark tint of brown-green, that it would appear black.

Opacifier :not found – glass is appears black and translucent.

Evidences of recycling:none

Other:Enriched in Rb, while significantly depleted in Sr, amounts of Th and U are more than 10 times .higher compared to other glass fragments.

Fragment 098_001

Object: a base

Type of glass: Heavily altered natron soda-lime glass, that appears as forest glass in ternary plot, because of a surface layer depleted in sodium

Colorants and decolorants: Cu in aquantity of 1416,00ppm as well as 170 ppm of Co creating another the striking blue colour to appear.

Opacifier : not found, probably translucent under the altered layers.

Evidences of recycling: not found

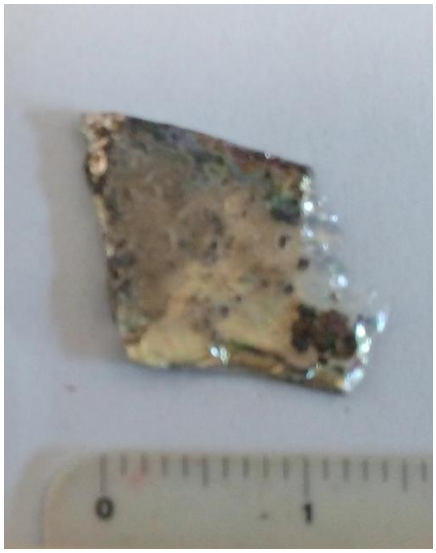

Fragment 098_004

Object: a rim

Type of glass: Heavily altered natron soda-lime glass, that appears as forest glass in ternary plot, because of a surface layer depleted in sodium

Colorants and decolorants: Cu in quantity of 840ppm as well as 39,6 ppm of Co should have caused a blue color, as it did not happen a decolorant in a large quantity should have been used, which already confirms recycling.

XRF analysis shows a huge amount of iron 1373 counts and even higher levels of manganese – 2090 counts

Very high amount of MnO – 6,18%

Opacifier : Antimony concentrations could increase the opacify of the sample

Evidences of recycling:High levels of Baand Pb measured in thousands ppm were detected, as well as 385ppm of Sb.

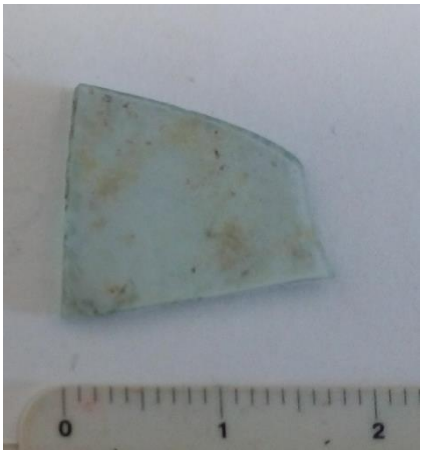

Fragment 36104_003

Object: a rim

Type of glass: Natron soda-lime glass

Colorants and decolorants: Light blue tint may have been caused by relatively low amount of Fe. Mn is in very low quantities 0,03%.

Opacifier : none

Evidences of recycling:none

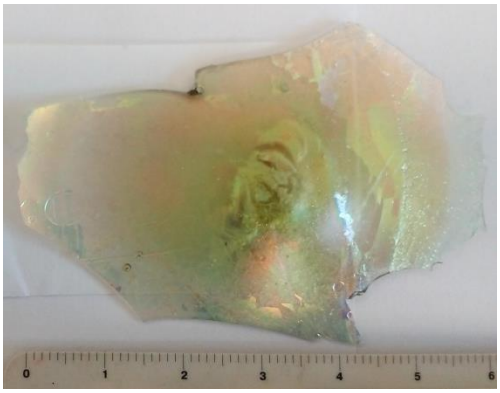

Fragment 36108_001

Object: a base of a glass vessel
Type of glass: Natron soda-lime glass
Colorants and decolorants: Yellowish hue caused by presence of Fe ions.
1,36% of Mn indicates deliberate adding to the glass batch.
Opacifier : none
Evidences of recycling: 348ppm Pb and 187 ppm of Sb

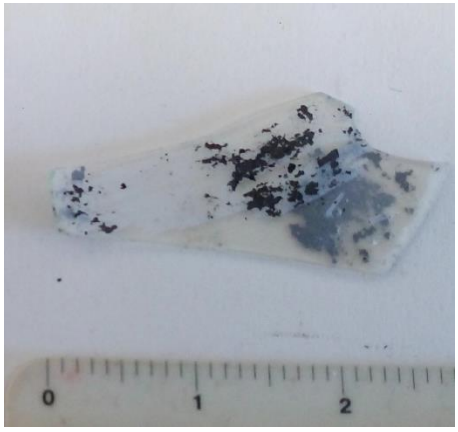

Fragment 36192_001

Object: a part a wall of a glass vessel

Type of glass: Natron soda-lime glass

Colorants and decolorants: Glass looks colourless because of the 1% of Mn compared to lower amounts of Fe.

Opacifier : none

Evidences of recycling:none

As this study shows, Mn is present in almost every glass sample of that time period. Howerer, for the author was interesting to know is there is any strong correlation between another element, which would indicate that they came from the same source.

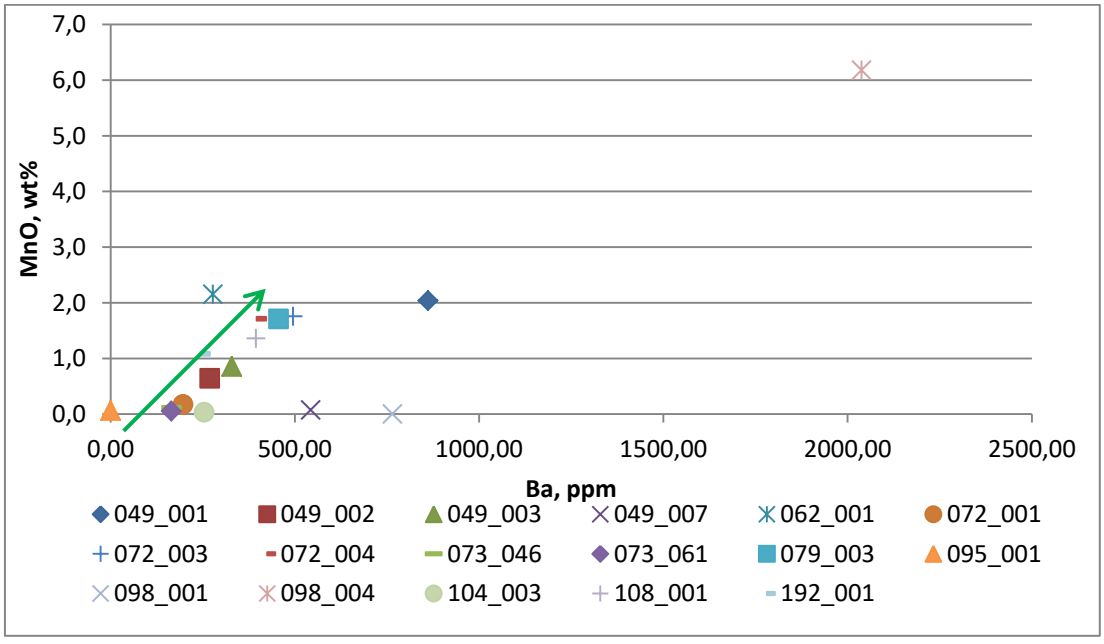

Fig.14 MnO and Ba correlation

Roman natron glasses decoloured by Mn often show elevated Ba contents and a positive correlation between Mn and Ba. It is constant with the use of a mix of pyrolusite (MnO_2) and psilomelane ($(Ba,H_2O)_2Mn_5O_{10}$) as the source of Mn[14]. The abovementioned positive correlation is observed in the fragments analyzed in this study as well.

The data on rare earth elements obtained by LA-ICP-MS technique can contribute to the provenance study of the fragments. A spider-diagram of all 18 analyzed fragments normalized to chondrite REE values in order to obtain an information about glass provenance is shown on the Fig. 15

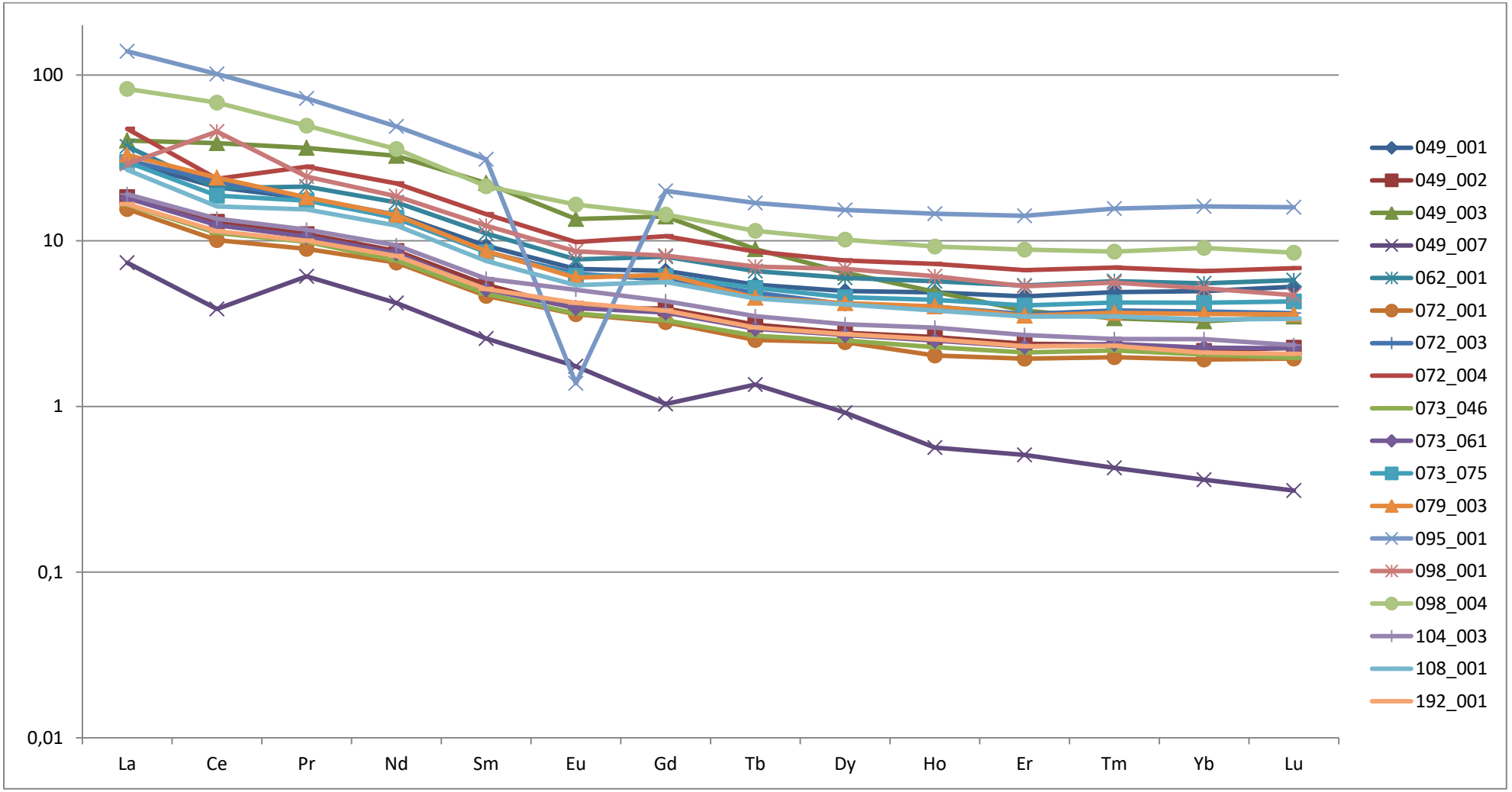

Fig 15. A spider-diagram of REE of 18 fragments analyzed by LA-ICP-MS normalized to chondrite REE values

A closer look on the obtained REE patterns reveals to a researcher that there are some differences between them. On such a diagram a difference in patterns means a different source of raw materials, and vice versa, when the REE profiles of the samples look parallel or undistinguishably similar, it raises the probability of glass production materials coming from the same place(s). It can be clearly seen, that the prevalent majority of the samples have almost the same REE profile, and this not doubtful similarity is shown on the Fig.16, (non-similar patterns are excluded).

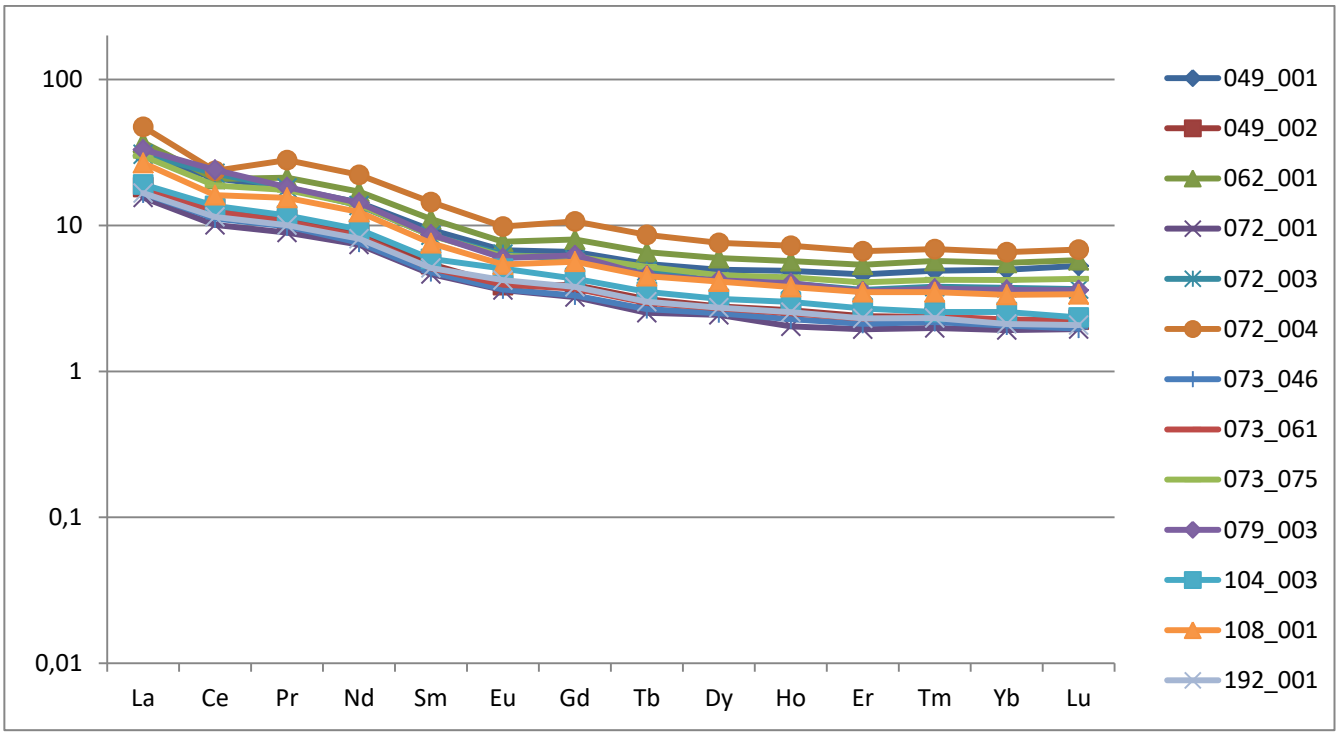

Fig. 16 A spider-diagram (normalized by chondrite REE values) of fragments with a similar/the same pattern of rare earth elements.

There are some key points about the similarities of the patterns, that the author would like to highlight. First of all, it is the fact that Eu-negative anomaly looks quite subtle and almost cannot be seen. Secondly, the slight depletion in Ce can be seen. Thirdly, the light rare earth elements have higher values and are gradually depleting in values towards the heavy REE, them. Finally, the heavy REE are having similar values between themselves, which results in a plateau on the REE plot.

However, even if the diagram indicates it, one cannot be absolutely sure that all of the raw materials come from the same places as REE patterns of Roman soda-lime glass look quite similar to each other.

In order to compare the rest of the REE patterns to the main one, but to not overcrowd the resulting diagram, it was decided to calculate main values of each of rare earth elements of the samples with the same pattern. The resulting average-valued “main” pattern has been plotted together with the five dissimilar ones on the Fig.

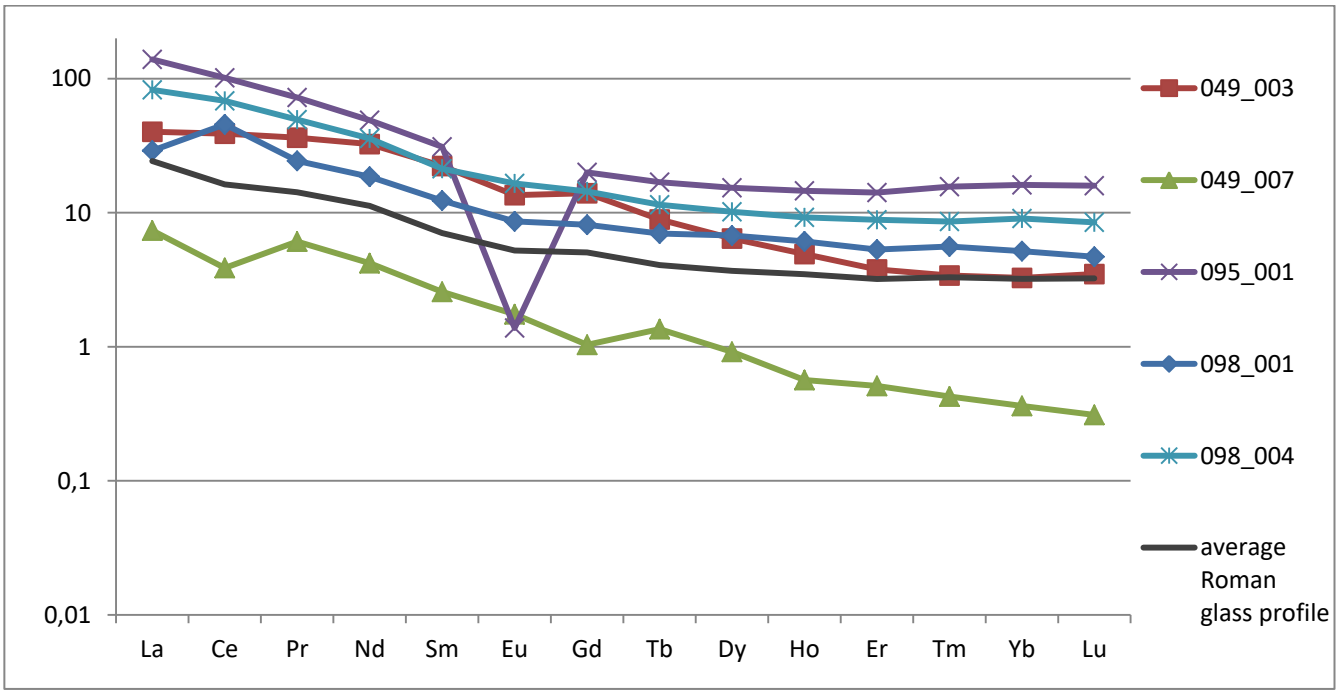

Fig. A spider-diagram (normalized by chondrite REE values) of fragments with different patterns of rare earth elements compared to our average-valued "main" profile

One can easily observe that glass fragments 095_001 and 049_007 are distinguishably dissimilar to the rest of the fragment patterns, while a pattern of a fragment 049_003 varies from the majority of the samples' patterns only slightly.

Probably the easiest thing to note on the diagram, it is the strong V-shaped Eu-negative anomaly seen in the pattern of the sample 095_001 and the fact that the values of all the REE except Eu are much higher than the average REE profile.

When taking a closer look on a sample 049_007, the main differences are the absence of Eu-anomaly, slight depletion in Ce values, generally lower levels of all the REE and the absence of a plateau in heavy REE. A pattern of a fragment 049_003 can be characterized by these key points: similar values of light REE with a minor Eu-negative anomaly and the absence of a plateau in heavy REE.

Regarding the fragment 098_004, its REE are gradually depleting in values onto a plateau, creating a "smoother" profile in comparison to our "main" profile.

Lastly, the fragment 098_001 has a higher amount of Ce then the rest of REE and much higher Ce values compared to our average-valued profile.

All the features described above are important to note as they are the evidence of the usage of different raw materials for the glass production.

7. Conclusions

From the start this study was quite ambitious even in the number of the artifacts analyzed. And it is one of the first attempts to obtain some answers from a limited amount of techniques that are allowed to use, because of the historical value of the glass fragments.

It was estimated that not all of the fragments were produced in the same way, and that raw materials used were the same for a one period in time (all of the stratigraphic layer 36073), and then they start to differ. The prevailing type of glass, as expected, was Roman natron (soda-lime) glass. However, the data obtained from five samples 049_003, 049_007, 095_001, 098_001, 098_004 inclines that it is not only used different raw materials for the glass production, but also that it appears to be a different type of glass. However, for fragments 098_001, 098_004 the author suggests, that they are indeed natron soda-lime glasses, with a thick altered layer, that is depleted in sodium. The fragment 095_001 appears to be different from any other glass fragments analyzed, in its major elements, in REE and in traces as well. It is possible to suggest that being the fragment 095_001 is the only one representative of mixed-alkali glasses.

The archaeometric study of each of the 18 fragments analyzed with both XRF and LA-ICP-MS have found vivid evidences of glass recycling, based on the ppm levels of Pb and Sb as well as MnO wt%. Which showed that10 out of 18 studied fragments have been, indeed, recycled.

The study of colorants used in this glass assemblage indicates mostly the usage of Fe, however, mostly without intention, resulting in an aqua or yellowish tint of the resulting glass. For the colorless glasses Mn and Sb were used is most of the cases, and given the amounts used, it can be said that it was intentional (knowing that its introduction to the glass batch will result in obtaining a colorless glass). For the blue glass, Cu and Co were used a colorants. However, the glasses with relatively average amounts of Cu and Co were colorless, when Mn and Sb were present in higher amounts, which also supports the previous evidences that the glass fragments studied were recycled.

Even if the origin of the raw materials of the glass fragments was not determined geographically, the data obtained by LA-ICP-MS and XRF techniques contributed to the knowledge of the composition of Roman glasses, their patterns of Rare Earth elements and recycling of the glasses in the beginning of the Middle Ages in Rome.

The huge database of glass elemental composition created during this study are a good basis for further studies of the Roman glasses.

Bibliography

1) K. Janssens, Ed., *Modern Methods for Analysing Archaeological and Historical Glass*. Chichester: Wiley, 2013.
2) M. A. Pollard and C. Heron, *Archaeological Chemistry*, vol. 1. Cambridge: The Royal Society of Chemistry, 2008
3) G. Artioli, *Scientific methods and cultural heritage: an introduction to the application of materials science to archaeometry and conservation science*. Oxford: Oxford University Press, 2012.
4) Jackson, C. M., H. E. M. Cool, Wager, E.C.W.,. *The manufacture of glass in Roman York.* Journal of Glass Studies 40, 55-61,1998
5) Freestone, I. C., *Glass production in Late Antiquity and the Early Islamic period: a geochemical perspective*. Geomaterials in Cultural Heritage, Geological Society of London. Special publication 257: 201-216, 2006
6) Stern, E. M., *Roman Glassblowing in a Cultural Context*. American Journal of Archaeology 103/3, 441-48. 1999
7) Jackson, Caroline M. "Making colourless glass in the Roman period." *Archaeometry* 47.4 (2005): 763-780.
8) Freestone, I.C., 2008. Pliny on Roman Glassmaking. In: Matinón-Torres, M., Rehren, T.(eds.) *Archaeology, History and Science. Integrating Approaches to Ancient Materials* (UCL Institute of Archaeology Publications), Oxford, 77-100.
9) Lucas, A., 1932. The Occurrence of Natron in Ancient Egypt. *J. Egypt. Archaeol.* 18, 62–66.
10) Shortland, A.J., 2004. Evaporites of the Wadi Natrun: seasonal and annual variation and its implication for ancient exploitation. *Archaeometry 46*, 497-516.
11) Shortland, A.J., Schachner, L., Freestone, I.C., Tite, M., 2006. Natron as a flux in the early vitreous materials industry: sources, beginnings and reasons for decline. *Journal of Archaeological Science* 33, 521-530
12) Carandini, A., & Carafa, P. (Eds.). (2017). *The atlas of ancient Rome: biography and portraits of the city*. Princeton University Press.
13) Giussani, Barbara & Monticelli, Damiano & Rampazzi, Laura. (2009). Role of laser ablation-inductively coupled plasma-mass spectrometry in cultural heritage research: A review. Analytica chimica acta. 635. 6-21. 10.1016/j.aca.2008.12.040.
14) Degryse, Patrick, ed. Glass making in the Greco-Roman world: results of the ARCHGLASS project. Vol. 4. Leuven University Press, 2015

15) Velde, B., and Gendron, C., 1980, Chemical composition of some Gallo-Roman glass fragments from central western France, *Archaeometry*, 22, 183–7.
16) Freestone, I. C., Bimson, M., and Buckton, D., 1990, Compositional categories of Byzantine glass tesserae, in *Annales du 11e Congrès de l'Association Internationale pour l'Histoire du Verre, Bâle, 29 août—3 septembre1988*, 271–81, AIHV, Amsterdam.
17) Mirti, P., Casoli, A., and Appolonia, L., 1993, Scientific analysis of Roman glass from Augusta Praetoria, *Archaeometry*,35, 225–40.
18) Fleming, S., 1999, *Roman glass: reflections on cultural change*, University of Pennsylvania Museum of Archaeology and Anthropology, Philadelphia, PA
19) Sayre, E. V., 1963, The intentional use of antimony and manganese in ancient glasses, in (eds). Advances in glass technology, part 2 (eds. F. R. Matson and G. Rindone), 263–82, Plenum Press, New York.
20) Sayre, E. V., and Smith, R. W., 1967, Some materials of glass manufacturing in antiquity, in Archaeological chemistry: a symposium (ed. M. Levey), 279–311, University of Pennsylvania Press, Philadelphia, PA.
21) Smith, R. W., 1971, The analytical study of glass in archaeology, in Science in archaeology: a survey of progress andresearch (eds. D. R. Brothwell and E. Higgs), 614–24, Thames and Hudson, London.
22) Pliny, *Natural History*, 36.112
23) Battistelli 2001
24) Marella Vianello 1950 (p21-32)
25) Carandini, Bruno, Fraioli 2010
26) Plutarch, Life of Caesar, 12.1
27) Carandini, Papi 2005
28) Anselmino 2006
29) Ovid, *Fasti*, 4,347
30) Pensabene et al. 2006
31) Cicero, *On His House*, 115; idem, *On the Response of the Haruspies*,30
32) Pliny, *Natural History*, 36.7-8, 36.114-15.
33) Pliny, *Natural History*, 36.103
34) Ovid, *Fasti* 4.347-48.
35) Ovid, *Fasti* 4.952; idem, Metamorposes, 15.865
36) Plutarch, Life of Antony, 54.2, 57.4-5.
37) Cassiis Dio, 53.27.5.
38) Statius, Silvae, 3,3.67

39) Panella 2011b, Nerone e il grande incendio del AD 64, p76-91
40) Martial, 8.36
41) Filippo Coarelli 2009b, p86-87
42) Pensabene and Coletti 2006, pages 534-86.
43) Carboni 2011, page 146
44) Parlini, Gabriela *Horreum vespasiani, ambiente 108. La stratigrafia e i reperti delle fasi 1-7.*, 2018
45) Brouwer , Peter. "Theory of XRF". Almelo, Netherlands:PANalytical BV, 2006
46) Detlef Günther, Bodo Hattendorf, Solid sample analysis using laser ablation inductively coupled plasma mass spectrometry, TrAC Trends in Analytical Chemistry,Vol. 24, Issue 3,2005, p255-265
47) Dussubiex, L, Golotko, M., & Gratuze, B(eds.) (2016) resent advantages in laser ablation ICP-MS for archaeology. Berlin: Springer.
48) Angelini, Ivana, et.al. "Chemical analyses of Bronze Age glasses from Frattesina di Rovigo, northern Italy.' Journal of Archaeological Sciene 31.(8) 1175-1184"
49) Keiga Kawaguchi, et al. Accelerated formation of sodium depletion layer on soda lime glass surface by corona discharge treatment in hydrogen atmosphere, Applied Surface Science, Vol. 300, 2014, p149-153,

Annex

Table LA-ICP-MS Quality Control (NIST 610)

	SiO2	Na2O	MgO	Al2O3	P2O5	K2O	CaO	TiO2	MnO	FeO
NIST610-85	70,4	14,0	0,1	1,9	0,1	0,1	11,6	0,1	0,1	0,1
NIST610-85	70,5	13,9	0,1	1,9	0,1	0,1	11,5	0,1	0,1	0,1
NIST610-85	70,6	13,9	0,1	1,9	0,1	0,1	11,5	0,1	0,1	0,1
NIST610-85	70,5	13,9	0,1	1,9	0,1	0,1	11,5	0,1	0,1	0,1
NIST610-85	70,2	13,9	0,1	1,9	0,1	0,1	11,8	0,1	0,1	0,1
NIST610-85	70,4	13,9	0,1	1,9	0,1	0,1	11,7	0,1	0,1	0,1
NIST610-85	70,3	13,9	0,1	1,9	0,1	0,1	11,7	0,1	0,1	0,1
NIST610-85	70,3	13,8	0,1	1,9	0,1	0,1	11,9	0,1	0,1	0,1

Table LA-ICP-MS Quality Control (BCR2G)

SelectionLabel	G_BCR2G_1	G_BCR2G_2
Li_ppm_m7	9,66	9,72
Li_ppm_m7_Int2SE	0,25	0,28
Li_ppm_m7_LOD	0,15	0,091
Be_ppm_m9	2,2	2,23
Be_ppm_m9_Int2SE	0,22	0,2
Be_ppm_m9_LOD	0,12	0,061
B_ppm_m11	5,5	5,08
B_ppm_m11_Int2SE	0,42	0,39
B_ppm_m11_LOD	0,54	0,58
Sc_ppm_m45	41,66	36,65
Sc_ppm_m45_Int2SE	0,77	0,6
Sc_ppm_m45_LOD	0,089	0,09
V_ppm_m51	410,7	409,1
V_ppm_m51_Int2SE	6,9	6,8
V_ppm_m51_LOD	0,051	0,062
Cr_ppm_m53	14,85	14,09
Cr_ppm_m53_Int2SE	0,65	0,72
Cr_ppm_m53_LOD	0,4	0,43
Co_ppm_m59	36,76	36,54
Co_ppm_m59_Int2SE	0,5	0,52
Co_ppm_m59_LOD	0,054	0,054
Ni_ppm_m60	12,37	11,98
Ni_ppm_m60_Int2SE	0,39	0,44
Ni_ppm_m60_LOD	0,13	0,14
Cu_ppm_m65	18,5	17,22
Cu_ppm_m65_Int2SE	1,1	0,44
Cu_ppm_m65_LOD	0,15	0,16
Zn_ppm_m66	156,5	141,5
Zn_ppm_m66_Int2SE	4,5	3,6
Zn_ppm_m66_LOD	0,2	0,2
Ga_ppm_m71	21,95	21,69
Ga_ppm_m71_Int2SE	0,42	0,48

Ga_ppm_m71_LOD	0,029	0,034
As_ppm_m75	1,18	0,642
As_ppm_m75_Int2SE	0,14	0,08
As_ppm_m75_LOD	0,43	0,14
Rb_ppm_m85	48,39	48,42
Rb_ppm_m85_Int2SE	0,78	0,82
Rb_ppm_m85_LOD	0,046	0,049
Sr_ppm_m88	342,2	343,5
Sr_ppm_m88_Int2SE	4,8	5,2
Sr_ppm_m88_LOD	0,0024	0,0025
Y_ppm_m89	32,5	32,12
Y_ppm_m89_Int2SE	0,5	0,42
Y_ppm_m89_LOD	0,0021	0,0042
Zr_ppm_m90	168,1	169,1
Zr_ppm_m90_Int2SE	2,8	2,3
Zr_ppm_m90_LOD		0,0083
Nb_ppm_m93	10,52	10,46
Nb_ppm_m93_Int2SE	0,21	0,2
Nb_ppm_m93_LOD		0,0035
Sn_ppm_m118	1,878	1,874
Sn_ppm_m118_Int2SE	0,072	0,087
Sn_ppm_m118_LOD	0,05	0,033
Sb_ppm_m121	0,49	0,34
Sb_ppm_m121_Int2SE	0,25	0,066
Sb_ppm_m121_LOD	0,1	0,19
Cs_ppm_m133	1,13	1,147
Cs_ppm_m133_Int2SE	0,038	0,036
Cs_ppm_m133_LOD	0,0069	0,0076
Ba_ppm_m137	646	646
Ba_ppm_m137_Int2SE	11	12
Ba_ppm_m137_LOD	0,019	0,033
La_ppm_m139	25,67	25,6
La_ppm_m139_Int2SE	0,36	0,4
La_ppm_m139_LOD	0,0019	0,0019
Ce_ppm_m140	51,11	50,79
Ce_ppm_m140_Int2SE	0,7	0,81
Ce_ppm_m140_LOD		
Pr_ppm_m141	6,33	6,24
Pr_ppm_m141_Int2SE	0,11	0,11
Pr_ppm_m141_LOD	0,0013	
Nd_ppm_m146	27,25	27,43
Nd_ppm_m146_Int2SE	0,48	0,47
Nd_ppm_m146_LOD	0,0077	0,011
Sm_ppm_m147	6,15	6,38
Sm_ppm_m147_Int2SE	0,2	0,18
Sm_ppm_m147_LOD	0,012	0,0091
Eu_ppm_m153	1,989	1,916
Eu_ppm_m153_Int2SE	0,065	0,057
Eu_ppm_m153_LOD	0,02	0,0026
Gd_ppm_m157	6,33	6,36
Gd_ppm_m157_Int2SE	0,2	0,2
Gd_ppm_m157_LOD		
Tb_ppm_m159	1,006	0,972
Tb_ppm_m159_Int2SE	0,034	0,031
Tb_ppm_m159_LOD	0,0013	

Dy_ppm_m163	5,98	5,92
Dy_ppm_m163_Int2SE	0,15	0,16
Dy_ppm_m163_LOD		
Ho_ppm_m165	1,209	1,218
Ho_ppm_m165_Int2SE	0,032	0,038
Ho_ppm_m165_LOD		
Er_ppm_m166	3,172	3,246
Er_ppm_m166_Int2SE	0,085	0,095
Er_ppm_m166_LOD	0,0037	
Tm_ppm_m169	0,479	0,456
Tm_ppm_m169_Int2SE	0,019	0,018
Tm_ppm_m169_LOD	0,0017	0,0013
Yb_ppm_m173	3,15	3,21
Yb_ppm_m173_Int2SE	0,14	0,14
Yb_ppm_m173_LOD	0,0079	0,008
Lu_ppm_m175	0,485	0,486
Lu_ppm_m175_Int2SE	0,019	0,021
Lu_ppm_m175_LOD		
Hf_ppm_m178	4,58	4,71
Hf_ppm_m178_Int2SE	0,13	0,12
Hf_ppm_m178_LOD	0,0044	
Ta_ppm_m181	0,726	0,71
Ta_ppm_m181_Int2SE	0,026	0,025
Ta_ppm_m181_LOD		
Pb_ppm_m208	10,46	10,25
Pb_ppm_m208_Int2SE	0,46	0,27
Pb_ppm_m208_LOD	0,01	0,013
Th_ppm_m232	5,81	5,76
Th_ppm_m232_Int2SE	0,13	0,12
Th_ppm_m232_LOD		
U_ppm_m238	1,719	1,704
U_ppm_m238_Int2SE	0,04	0,044
U_ppm_m238_LOD		